AD NUMBER

AD910168

LIMITATION CHANGES

TO:

Approved for public release; distribution is unlimited.

FROM:

Distribution authorized to U.S. Gov't. agencies only; Test and Evaluation; MAY 1973. Other requests shall be referred to Air Force Rocket Propulsion Laboratory, Office of Technical Information, Attn: DOZ, Edwards AFB, CA 93523.

AUTHORITY

afrpl ltr, 31 jan 1974

AFRPL-TR-73-29

RADAR ATTENUATION MEASUREMENTS OF SELECTED SOLID PROPELLANTS AND THE EFFECT OF ADDITIVES

L.G. ALTMAN, JR, CAPT, USAF

S.B. THOMPSON, CAPT, USAF

P.C. SUKANEK, LT, USAF

TECHNICAL REPORT AFRPL-TR-73-29

MAY 1973

AIR FORCE ROCKET PROPULSION LABORATORY

DIRECTOR OF SCIENCE AND TECHNOLOGY

AIR FORCE SYSTEMS COMMAND

UNITED STATES AIR FORCE

EDWARDS, CALIFORNIA

SECTION I

INTRODUCTION

Solid rocket exhausts absorb, reflect and diffract electromagnetic signals incident upon them. Severe signal attenuation may result in loss of guidance and control in missile systems in which an electromagnetic link with the missile is required. Detection may be facilitated by enlarged radar cross sections resulting from plume-signal interactions.

The development of advanced high energy solid propellants, which frequently produce aluminum oxide particles and substantial free electron densities in the exhaust plume, exacerbated these problems. Consequently, the need for theoretical models which predict plume signal interference during the weapons systems design phase has become essential. At AFRPL, efforts to develop economical, accurate, computerized models for prediction of radar attenuation and reflectivity have been underway for several years. Specific programs now operational at AFRPL are the AeroChem Axisymmetric Mixing with Non-equilibrium Chemistry Computer Program (AFRPL-TR-69-167) and A Computer Program to Predict Radar Cross Section of Exhaust Plumes (AFRPL-TR-69-182). The AeroChem program has recently been revised (AFRPL-TR-72-94) and now calculates plume properties considerably faster.

Project EPIC was initiated when the opportunity of "piggy-backing" radar attenuation measurements on an existing AFRPL Project (305901 AMB, Static Testing of Solid Propellants for Air Force Weapons Systems) was recognized. The static test project was concerned primarily with determining the ballistic performance of advanced solid propellants. This provided a static engine firing program in which radar attenuation measurements in the plume could be made. The attenuation data are used not only to evaluate the plume-signal interference for the particular propellants tested, but also to provide experimental data for comparison with the predictions of various attenuation models.

AFRPL-TR-73-29

RADAR ATTENUATION MEASUREMENTS OF SELECTED SOLID PROPELLANTS AND THE EFFECT OF ADDITIVES

Laurice G. Altman, Jr., Captain, USAF
Samuel B. Thompson, Captain, USAF
Peter C. Sukanek, Lieutenant, USAF

Technical Report AFRPL-TR-73-29

May 1973

AIR FORCE ROCKET PROPULSION LABORATORY
DIRECTOR OF SCIENCE AND TECHNOLOGY
AIR FORCE SYSTEMS COMMAND
UNITED STATES AIR FORCE
EDWARDS, CALIFORNIA

FOREWORD

This report is the third of a series dealing with Project 305901AMB, Exhaust Plume Interference Characterization Program (Project EPIC). It discusses the program's progress from August 1968 to May 1970. Technical Reports AFRPL-TR-68-165 and 219 examine previous results.

The authors wish to thank Lt Dayton Silver for his computer programming assistance; Russell Sage and Msgt Thomas Norton for improvements in hardware design and fabrication; William Sands for test supervision; Tully Becker, Gordon Wallman, Jesse Lazenby, Harlan Berhow, SSgt David Dinger, and William Sublette for their instrumentation work; Tom Glaze for engineering support; and Capt Roderick Donaldson for reviewing the report.

This report has been reviewed and is approved.

PAUL J. DAILY, Lt Colonel, USAF
Chief, Technology Division

ABSTRACT

The primary objective of Project EPIC was to characterize solid propellants with respect to radar attenuation by their plumes. This report presents transverse and diagonal radar attenuation data on four different solid rocket propellants: RHP-112, AAP-3318, UTP-11475 and AAB-3220. Transverse attenuation data for propellants containing each of nine different radar attenuation suppressants (Mo, B_4C, Cr_2O_3, $VOSO_4$, $CoSnO_3$, $PbCrO_3$, Pb, CuO, K_2SO_4) are also given.

TABLE OF CONTENTS

LIST OF ILLUSTRATIONS

LIST OF TABLES

NOMENCLATURE

AP	ammonium perchlorate
db	decibel
D_t	throat diameter
F	thrust
F.I.	fuel index
gHz	gigahertz (billion cycles per second)
Isp	specific impulse
P_c	chamber pressure
r_j	nozzle exit radius
T_e	theoretical exit plane temperature
x	distance from nozzle exit plane
ϵ	nozzle expansion ratio

SECTION I

INTRODUCTION

Solid rocket exhausts absorb, reflect and diffract electromagnetic signals incident upon them. Severe signal attenuation may result in loss of guidance and control in missile systems in which an electromagnetic link with the missile is required. Detection may be facilitated by enlarged radar cross sections resulting from plume-signal interactions.

The development of advanced high energy solid propellants, which frequently produce aluminum oxide particles and substantial free electron densities in the exhaust plume, exacerbated these problems. Consequently, the need for theoretical models which predict plume signal interference during the weapons systems design phase has become essential. At AFRPL, efforts to develop economical, accurate, computerized models for prediction of radar attenuation and reflectivity have been underway for several years. Specific programs now operational at AFRPL are the AeroChem Axisymmetric Mixing with Non-equilibrium Chemistry Computer Program (AFRPL-TR-69-167) and A Computer Program to Predict Radar Cross Section of Exhaust Plumes (AFRPL-TR-69-182). The AeroChem program has recently been revised (AFRPL-TR-72-94) and now calculates plume properties considerably faster.

Project EPIC was initiated when the opportunity of "piggy-backing" radar attenuation measurements on an existing AFRPL Project (305901 AMB, Static Testing of Solid Propellants for Air Force Weapons Systems) was recognized. The static test project was concerned primarily with determining the ballistic performance of advanced solid propellants. This provided a static engine firing program in which radar attenuation measurements in the plume could be made. The attenuation data are used not only to evaluate the plume-signal interference for the particular propellants tested, but also to provide experimental data for comparison with the predictions of various attenuation models.

The Exhaust Plume Interference Characterization Program consisted of three phases: Traversing Transverse Attenuation Measurements, Diagonal Attenuation Measurements and Radar Additive Test Study (RATS).

The traversing attenuation measurements serve a dual purpose. First, they satisfy the primary objective of the project, the characterization of advanced solid propellants with respect to radar attenuation by their plumes. Second, the data may be used in refining plume models which predict transverse radar attenuation.

The second phase of Project EPIC consisted of diagonal attenuation measurements. These meausrements provide a more realistic assessment of plume signal interference because they were made with unfocused radar signals at aspect angles typical of air-launched missile mission scenarios.

The third phase, Radar Additive Test Study, consisted of a relatively low-cost technique of screening radar attenuation suppressant additives. Various additives were mixed with typical propellants containing different amounts of Al and AP. The propellant was fired, and the transverse attenuation measured. Results of the most recent portion of the additive study are presented in Section IV of this report.

Details of test configurations, further background information on Project EPIC and previously published radar attenuation data may be found in two previous reports, AFRPL-TR-68-165 and 219.

In the following three sections, each phase of the program is discussed. The purpose of this report is only to publish the experimental data for use in the technical community. No attempt at analysis of the data has been made.

SECTION II

TRAVERSING ATTENUATION MEASUREMENTS

Apparatus

A traversing radar system was used to determine transverse X- (9 gHz) and K- band (24 gHz) radar attenuation as a function of distance from the exit plane of the motor. The test equipment is shown in Figures 1 and 2. The radar horns were mounted on a moveable cart. When the motor was ignited, the cart was driven at constant speed along the plume axis. A more detailed description of the apparatus can be found in AFRPL-TR-68-165.

The radar lens was focused on the plume axis to a spot size of approximately 9 and 3.5 inches in diameter for the X- and K- band, respectively. A diagram of the radar components is given in Figure 3, with the components identified for each system in Table I. The system was calibrated prior to each test. Data were recorded on oscillographs and digital tape.

Four different motors were used in this study. The basic configuration is illustrated in Figure 4a. The nozzle shown here has a convergence angle of 45 degrees. Two other nozzles, with convergence angles of 15 degrees and 75 degrees, were also employed. The fourth motor had a submerged nozzle configuration as shown in Figure 4b.

Thirteen test runs for the purpose of determining the transverse attenuation were made. The test conditions are presented in Table II. All the tests were conducted at an optimum expansion ratio or were slightly under-expanded.

The compositions of four of the six propellants used in this study are given in Tabte III. The formulation of UTP-11475 is excluded since it is proprietary information. Propellant RHP-112 is a standard control propellant and its formulation may be found in the CPIA Solid Propellant Manual.

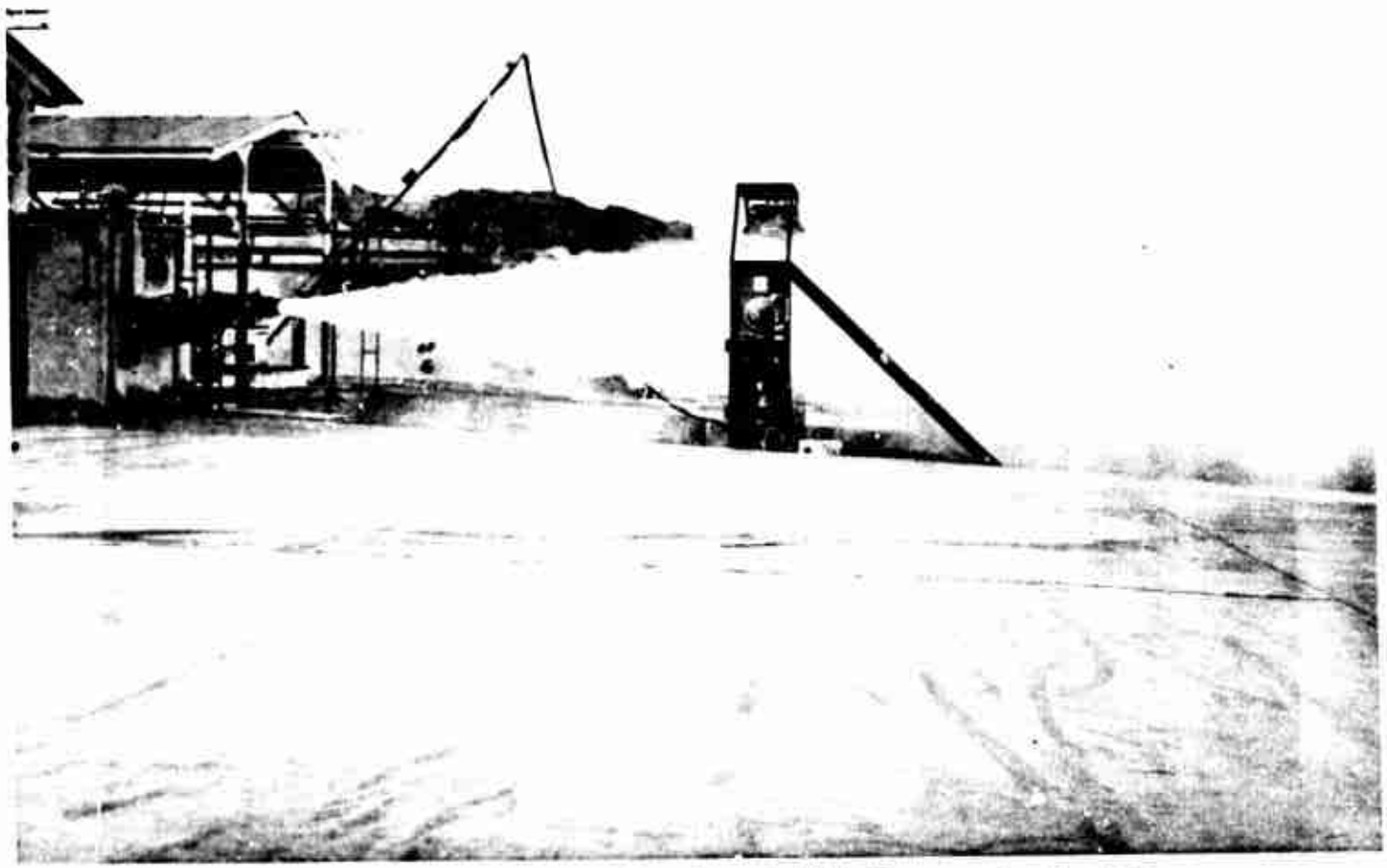

Figure 1. Static Test Monitored With Traversing System

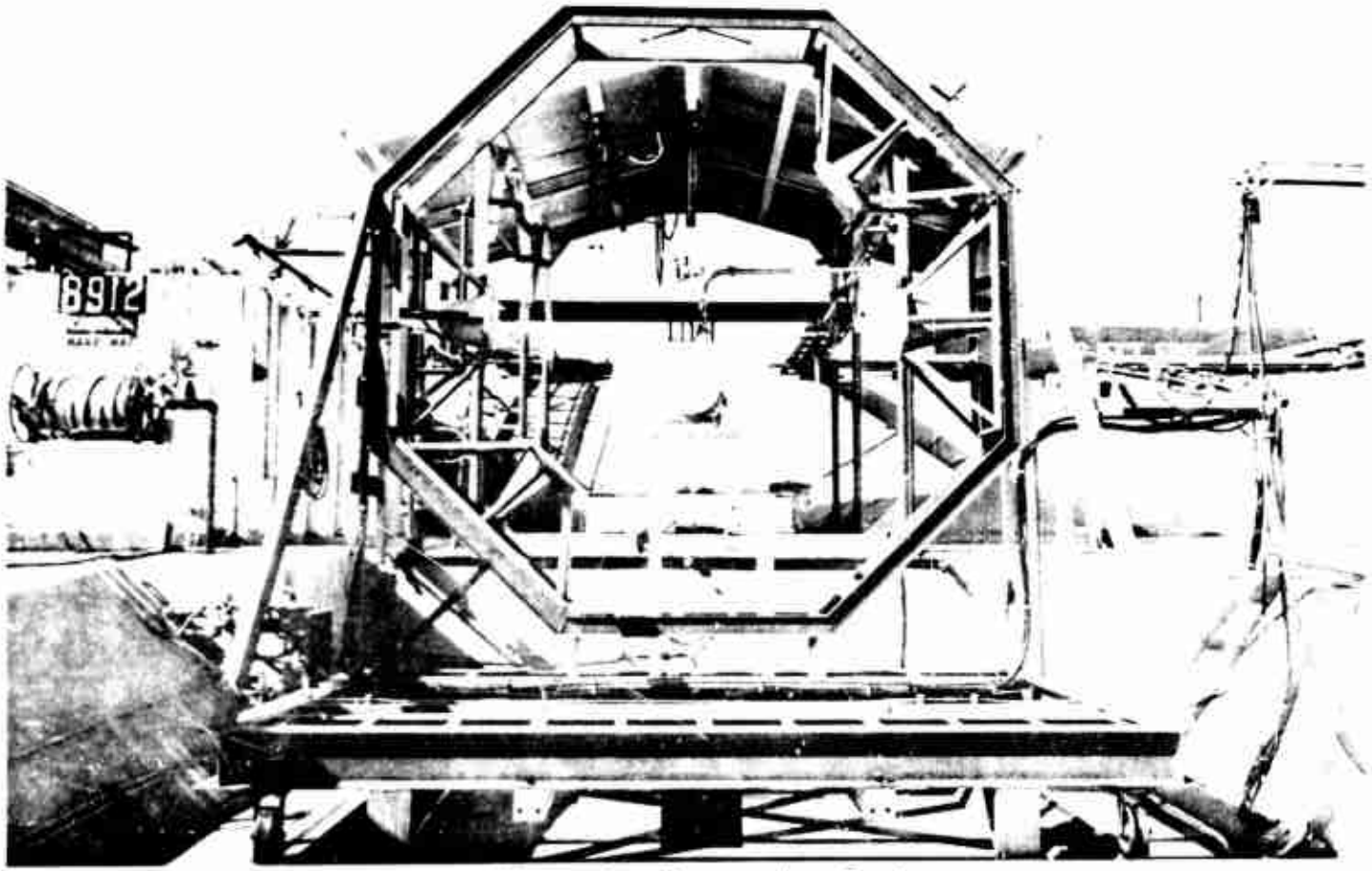

Figure 2. Traversing Cart

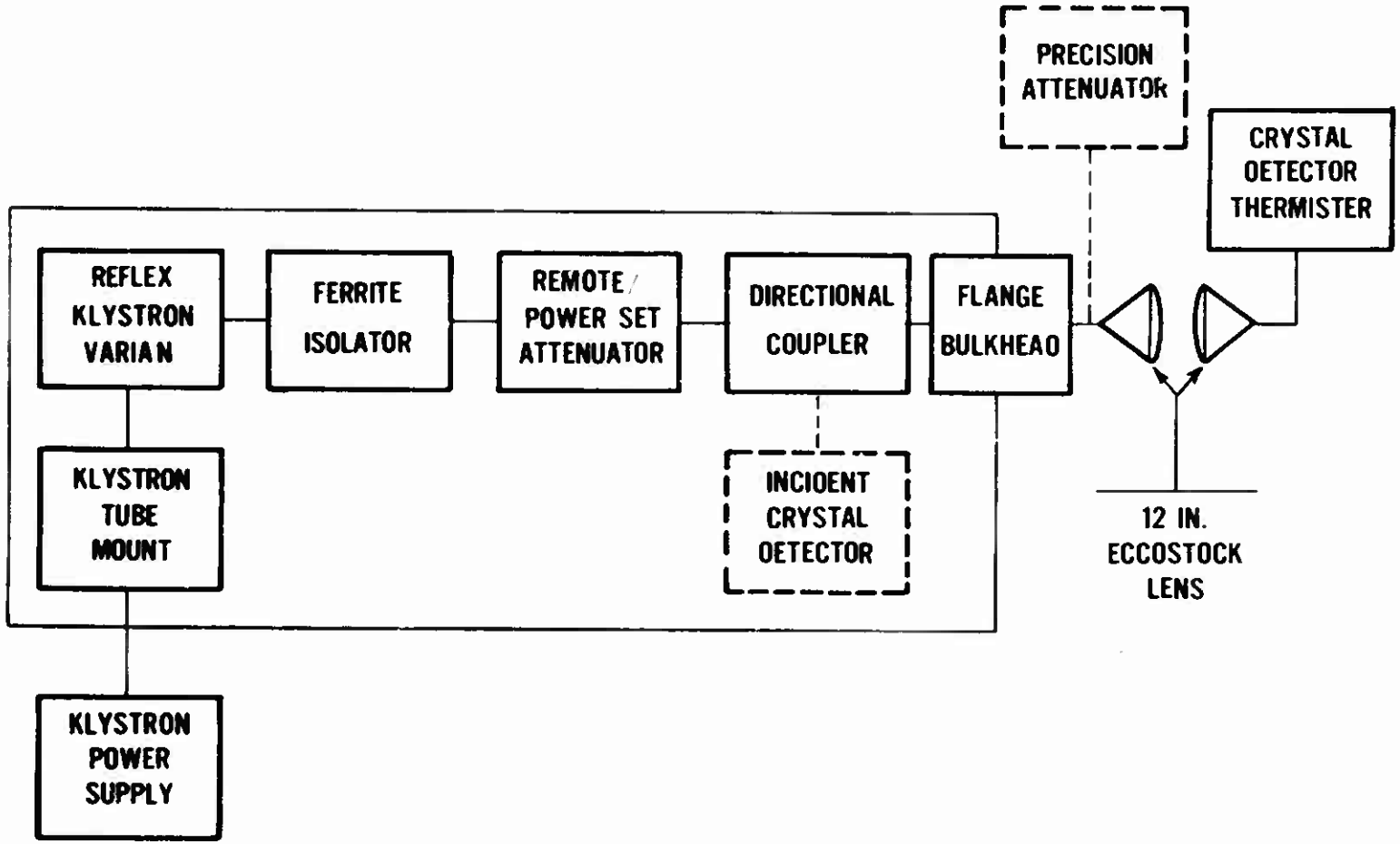

Figure 3. Radar System Diagram

TABLE 1. RADAR SYSTEM COMPONENTS

Component / System	X-Band Transversing	K-Band Transversing	Diagonal	RATS X-Band	RATS K-Band
Reflex Klystron Varian	MD-272	MD-1138	VA-272C	MD X-13	V-96
Ferrite Isolator	MD-1203	MD-1209	MD-1203	MD-1203	MD-1209
Power Set Attenuator	---	---	---	MD-47X2	DBE-410
Directional Coupler	MD-276F	MD-2770	DBG-X-279	DBG-X-279	DBX-279
Flange Bulkhead	---	DBE-275	DBG-275	DBG-275	DBE-275
Precision Attenuator	---	---	X-164AS	X-164AS	K-164AF
Klystron Tube Mount	MD-990	MD-2765	MD-990	MD-990	MD-990
Klystron Power Supply	HP-716B	HP-716B	HP-716B	HP-716B	HP-716B
Incident Crystal Detector	X-424A	K-422A	X-424	X-424A	---
Remote Attenuator	DBG-X-146	DBE-X-146	DBG-X-146	---	---
Crystal Detector	X-424A	K-422A	X-424(3)	X-424A	K-422A
Thermistor	11523A	11523A	---	11523A	11523A
12" Eccostock Lens	HT-0003	HT-0003	---	HT-0003	HT-0003

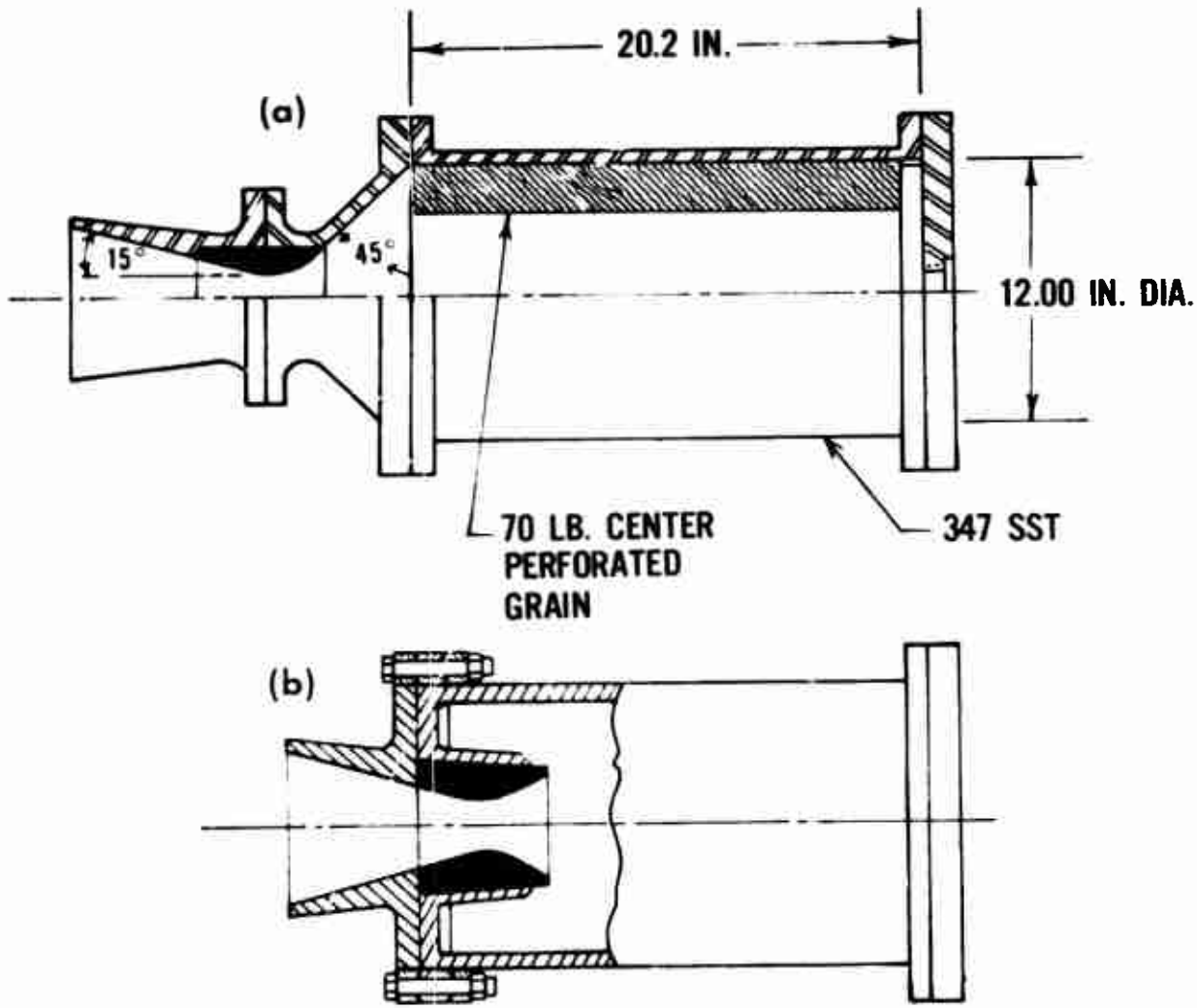

Figure 4. Nozzles Used in This Study: (a) Basic Configuration; (b) Submerged Nozzle

TABLE II. TEST CONDITIONS - TRANSVERSE ATTENUATION RUNS*

Propellant	Test	P_c (psi)	F (lb)	Fuel Index**	T_e† (°K)	D_t (in.)	r_j (in.)	ϵ	Nozzle Convergence Angle
RHP-112	1	1000	6035	0.63	1988	2.217	3.3	8.89	45°
RHP-112	2	1173	6443	0.63	1938	2.119	3.1	8.716	45°
RHP-112	3	977	5859	0.63	1997	2.213	3.3	8.895	15°
RHP-112	4	966	5749	0.63	2000	2.214	3.3	8.906	15°
RHP-112	5	978	5828	0.63	1996	2.210	3.3	8.870	75°
RHP-112	6	971	5882	0.63	1998	2.213	3.3	8.890	75°
RHP-112	7	1222	6624	0.63	---	2.090	3.1	8.762	45°††
RHP-112	8	1228	6626	0.63	---	2.087	3.1	8.797	45°††
AAP-3318	9	1278	4026	0.65	2096	1.603	2.4	8.814	45°
AAP-3318	10	926	3406	0.65	2187	1.775	2.6	8.732	45°
UTP-11475	11	898	2668	0.31	2668	1.542	2.3	8.33	45°
UTP-11475	12	1135	2875	0.30	2617	1.386	2.1	8.78	45°
UTP-11475	13	1161	2919	0.30	2617	1.384	2.1	8.90	45°

* A 70 lb test motor was used for all tests.

** Fuel Index = Mole ratio of combustible gaseous exhaust species (H, H_2, CO) to total gaseous species at nozzle exit plane; calculated from AFRPL Theoretical Isp Program.

† T_e = Theoretical temperature of exhaust gases at nozzle exit plane; taken from AFRPL Theoretical Isp Program.

†† Submerged nozzle.

TABLE III. PROPELLANT COMPOSITIONS

Ingredient	Weight %			
	AAP-3318	AAB-3220	RATS 7%	RATS 16%
Aluminum	20.0	16.0	7	16
Ammonium Perchlorate	58.0	50.0	77	68
Ammonium Sulfate	0.5			
Butylene Imine Adduct of Trimesic Acid		0.271		
Polybutadiene Binder		9.363		
Circo Light Oil (Napthenic Oil)			6	6
Guanidine Nitrate	4.0			
Isodecyl Pelargonate		4.20		
1, 2, 3-Tris (2 Methylaziridinyl) Phosphene Oxide		0.141		
Polybutadiene - Acrylic Acid Copolymer			10	10
Potassium Perchlorate		20.0		
Polyurethane C-1 Binder	17.0			
Silicon Oxide	0.5			
Zirconium Acetyl Acetonate		0.025		

Results

The transverse attenuation data for the thirteen test firings listed in Table II are presented in Figures 5 through 9. In all cases, the data have been smoothed using a Fourier series curve fitting technique. Figures 5 and 6 show the actual and smoothed data for X- band attenuation.

The data for the control propellant (RHP-112) used in the first eight firings of the static test project are given in Figures 5 nrough 8b. Figures 5 and 6 are for the nozzle with a 45 degree convergence angle; 7a and b, a 15 degree convergence angle; 7c and d, a 75 degree convergence angle; and 8a and b, the submerged nozzle configuration. These curves show that the maximum attenuation varies only slightly with the nozzle used.

Figures 8c and d show the transverse attenuation for propellant AAP-3318 fired from the nozzle with a 45 degree convergence angle. The data for propellant UTP-11475 are given in Figure 9. These were also taken with the nozzle with a 45 degree convergence angle.

The relatively low attenuation found here is attributed to the propellant's low level of combutible gaseous species at the motor exit plane. (The fuel index is approximately 0.30.)

A series of static tests was also performed with propellant AAB-3220. However, the attenuation exceeded the limits of the system (20 to 25 db). The plume was apparently seeded with alkali metal from a $KClO_4$ oxidizer. No transverse attenuation data are given.

The results of the thirteen tests are summarized in Table IV, where the maximum X- and K- band attenuation found in each test are given. Because of the limited amount of data available, it is difficult to draw any concrete conclusions concerning the effect of nozzle convergence angle,

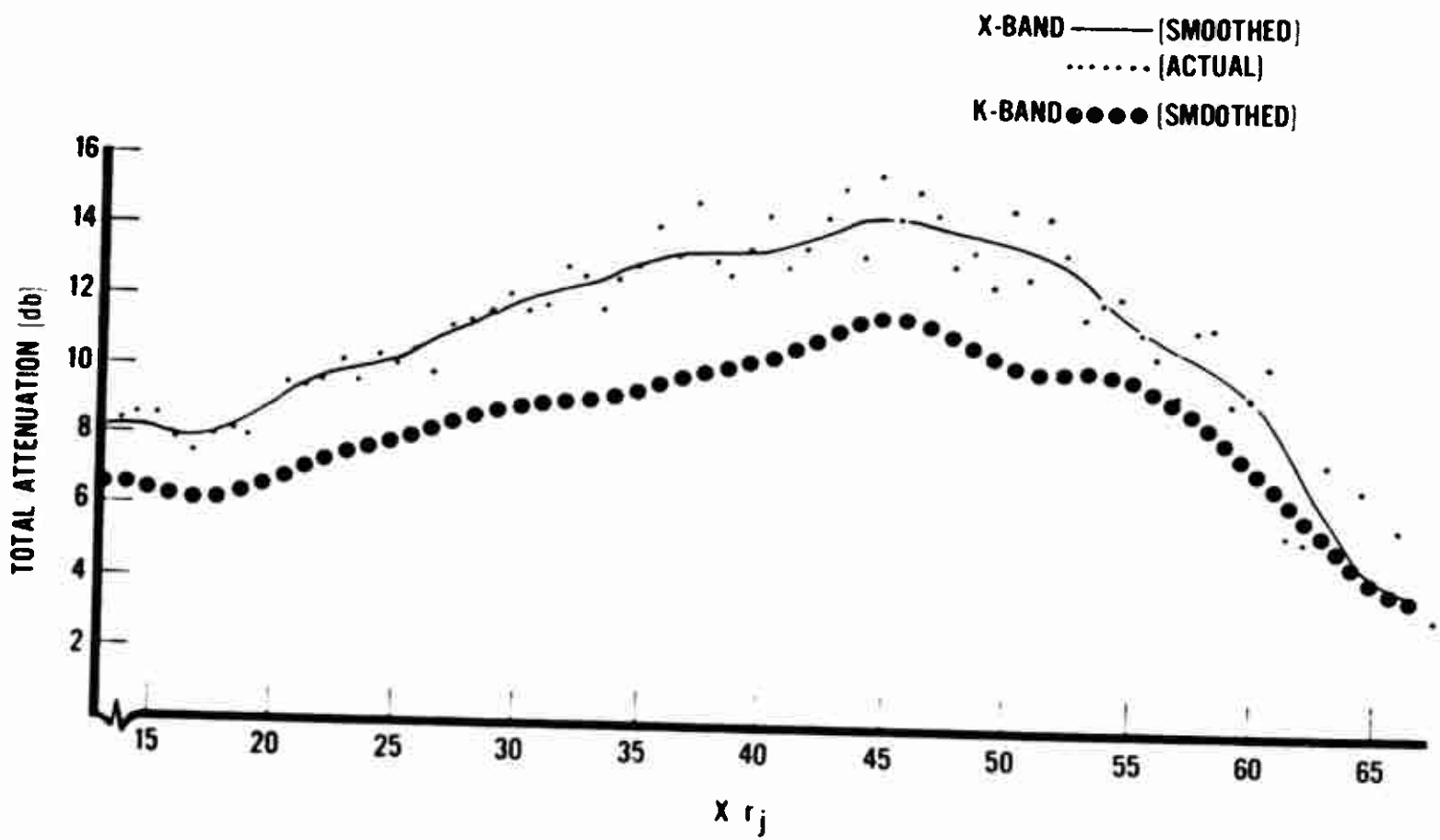

Figure 5. Test 1, Propellant RHP-112, X- and K- Band Attenuation

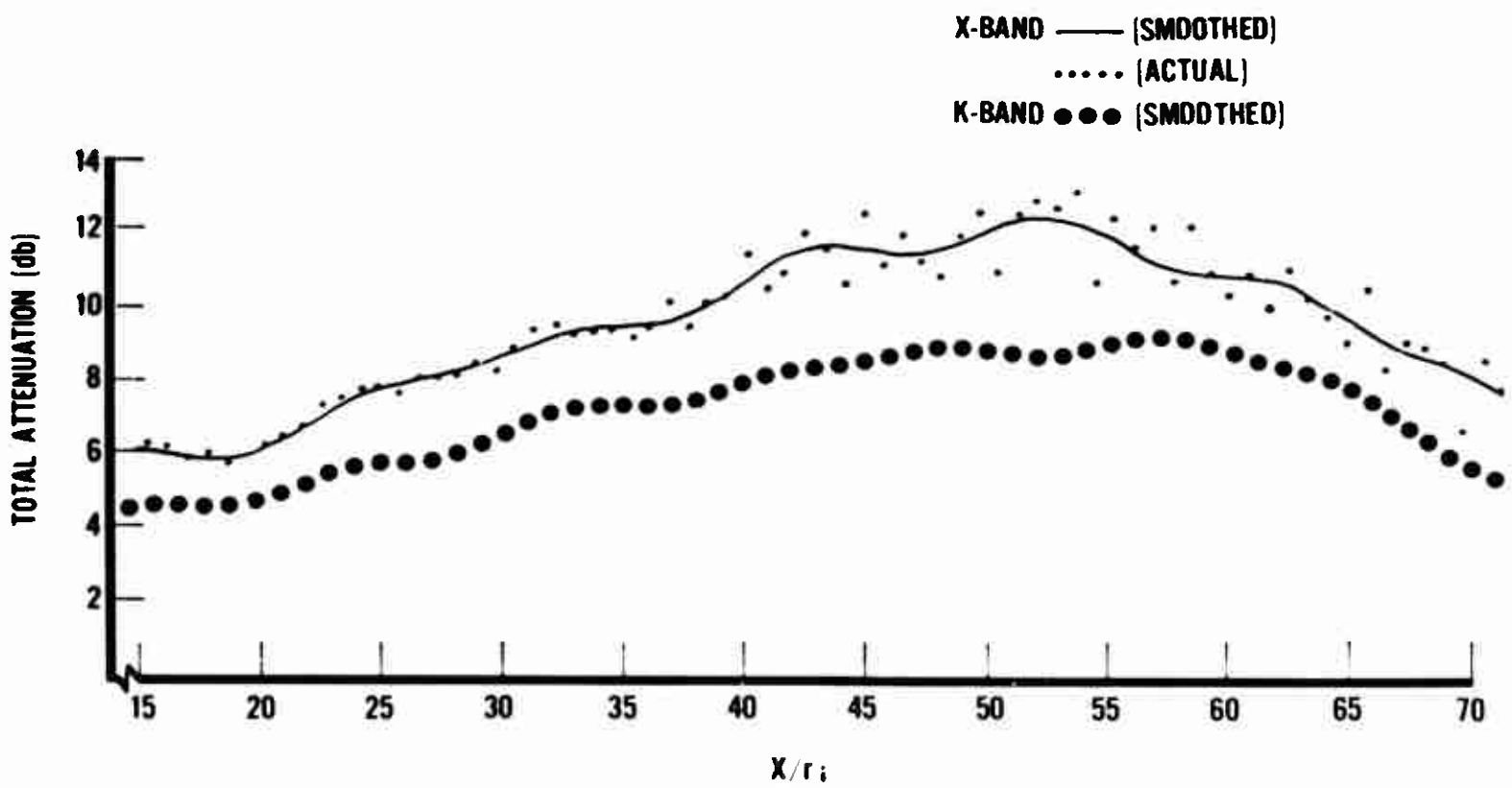

Figure 6. Test 2, Propellant RHP-112, X- and K- Band Attenuation

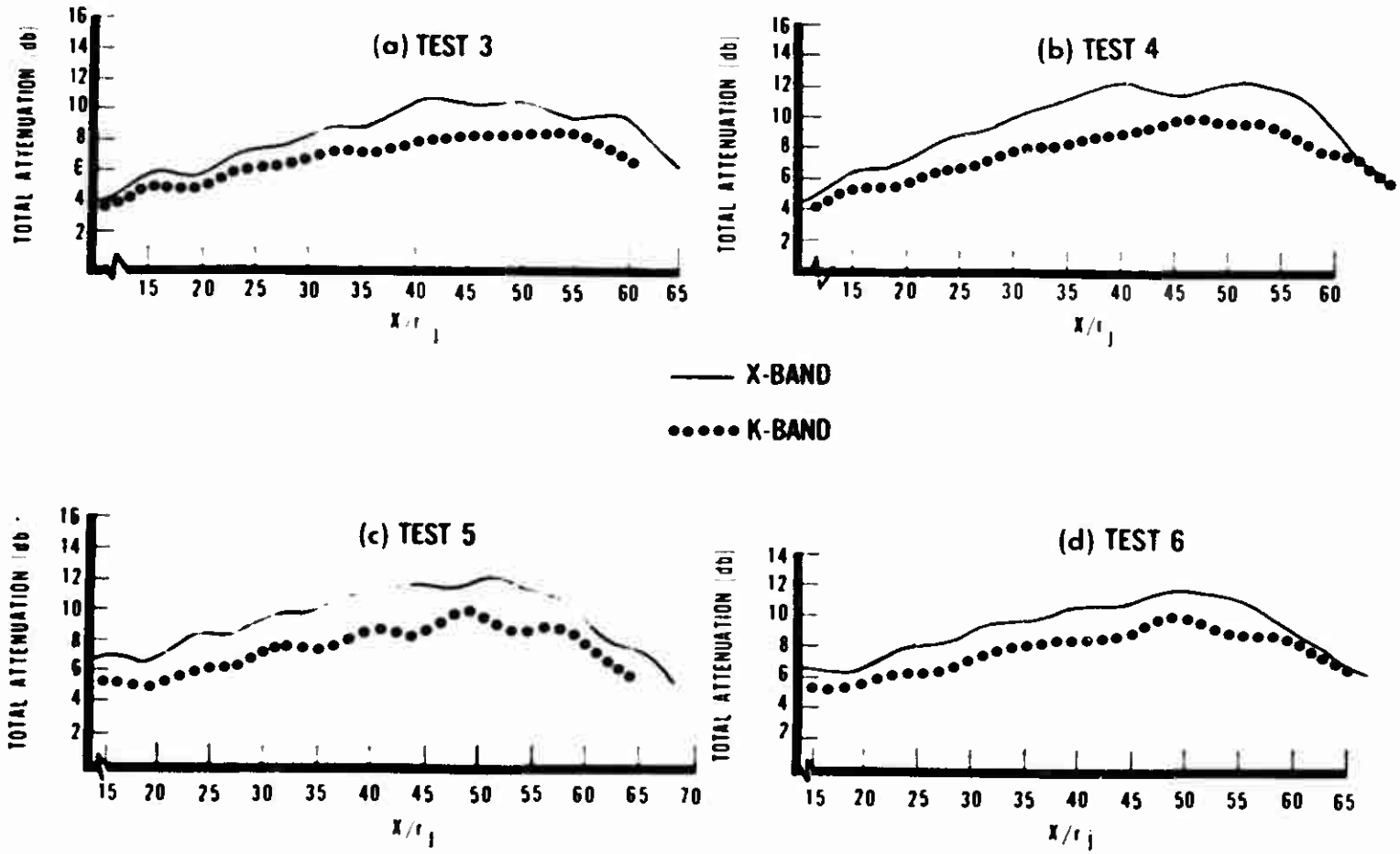

Figure 7. Propellant RHP-112, X- and K- Band Attenuation

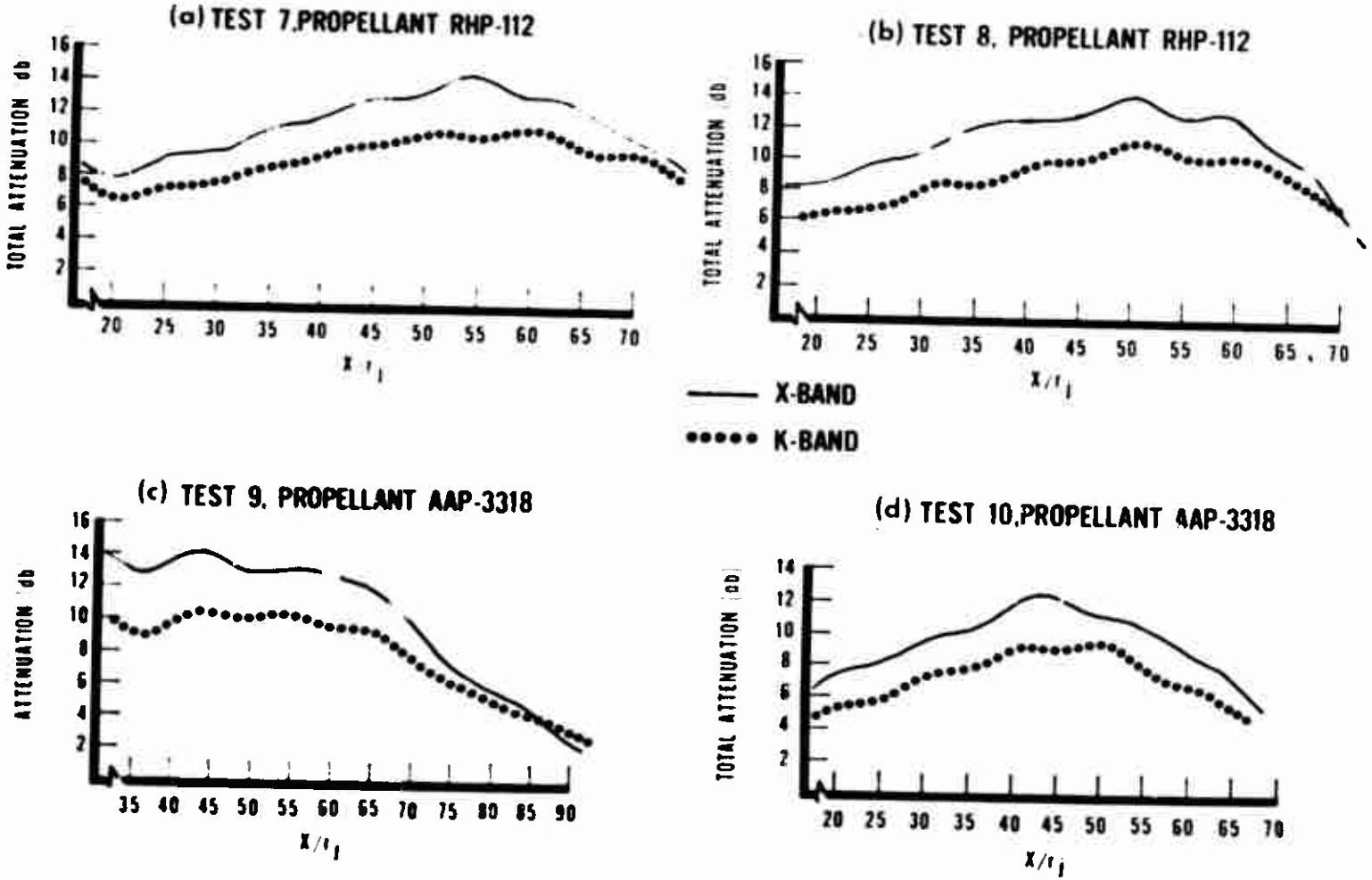

Figure 8. X- and K- Band Attenuation

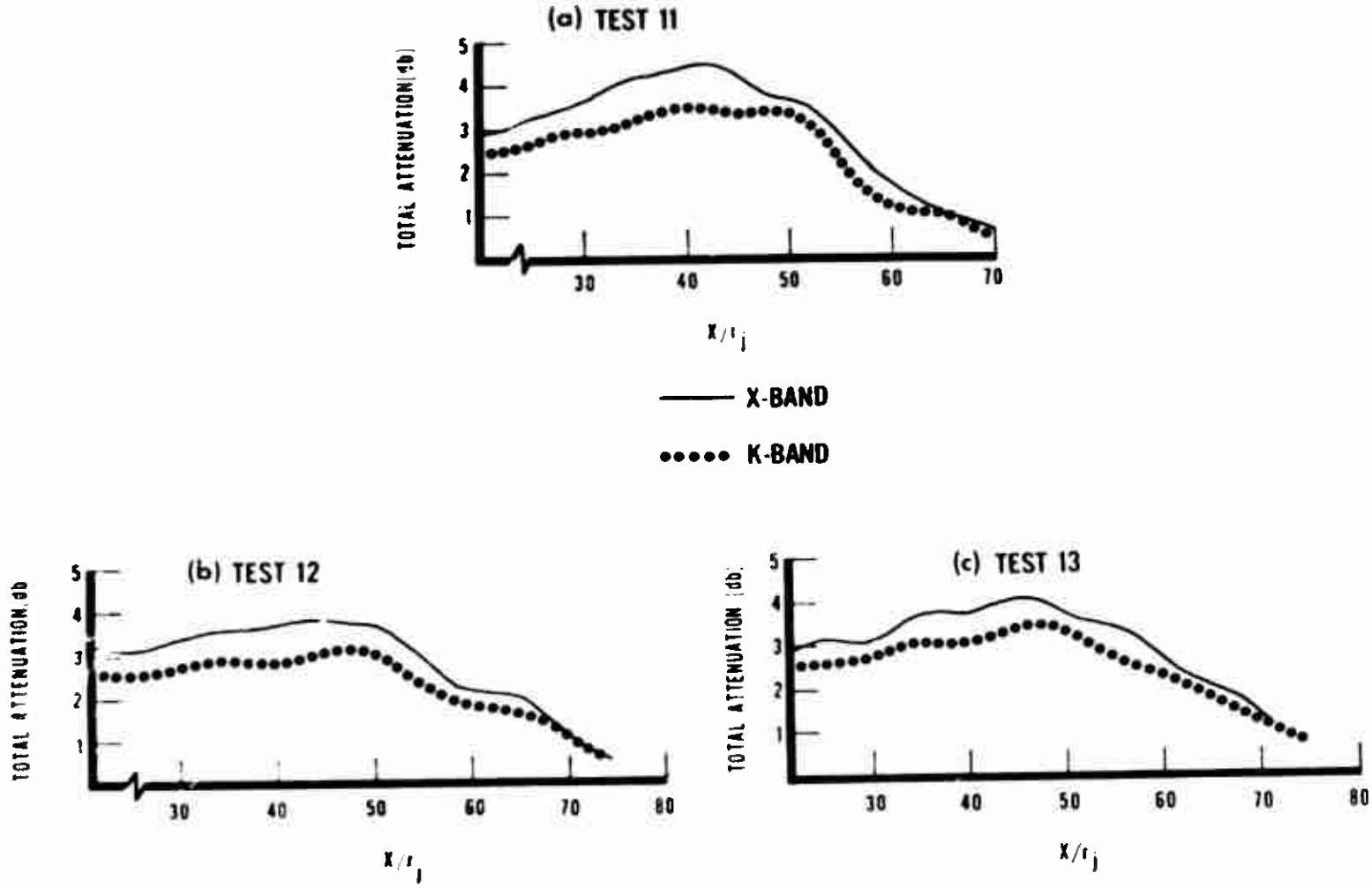

Figure 9. Propellant UTP-1475 X- and K- Band Attenuation

TABLE IV. MAXIMUM TRANSVERSE ATTENUATION

Propellant	Test	P_c (psi)	T_c (°K)	Nozzle Convergence Angle	Max Attenuation X-Band	Max Attenuation K-Band
RHP-112	1	1000	1988	45°	15	12
RHP-112	2	1173	1938	45°	13	9.5
RHP-112	3	977	1997	15°	11	9
RHP-112	4	966	2000	15°	12.5	10
RHP-112	5	978	1996	75°	12	10
RHP-112	6	971	1998	75°	12	10
RHP-112	7	1222	---	45°*	14.5	11.5
RHP-112	8	1228	---	45°*	14	11
AAP-3318	9	1278	2096	45°	14	10.5
AAP-3318	10	926	2197	45°	12.5	9.5
UTP-11475	11	898	2008	45°	4.5	3.5
UTP-11475	12	1135	2017	45°	3.8	3.1
UTP-11475	13	1161	2017	45°	4.2	3.5

* Submerged nozzle.

nozzle type, and chamber pressure on the attenuation through the plume. In general, the present data show that the maximum attenuation is essentially independent of these variables.

SECTION III

DIAGONAL ATTENUATION MEASUREMENTS

Apparatus

The diagonal attenuation measurement system is shown in Figure 10. The unfocused X-band transmitter horn is located at the nozzle exit plane, approximately 8 inches from the nozzle tip. The three receiver horns are located on an arc 32 feet from the transmitter horn at aspect angles of 14, 17 and 20 degrees with the plume axis and are designated A, B and C, respectively. The receiver horns are in the same horizontal plane as the plume axis and transmitter horn. The data are normalized with respect to horn sensitivity by individual calibrations prior to each test.

Results

Unfortunately, the static tests monitored with the diagonal radar system and those monitored with the traversing radar system were not conducted at the same chamber pressures. Furthermore, the static test project conducted firings using both the 70 lb motor, shown in Figure 4a, and a scaled down version of this motor, the 15 lb motor. The designation of 70 lb or 15 lb refers to the weight of center-perforated propellant cartridges used in the motor.

In spite of these limitations, the data in Table V are presented in consideration of their potential value in the development of diffraction models and sea level scaling.

In general, as the aspect angle of the transmitted signal increased from 14 to 20 degrees, the signal attenuation decreased approximately two decibels. This trend was reversed in the UTP-11475 series, which was conducted at significantly lower chamber pressures.

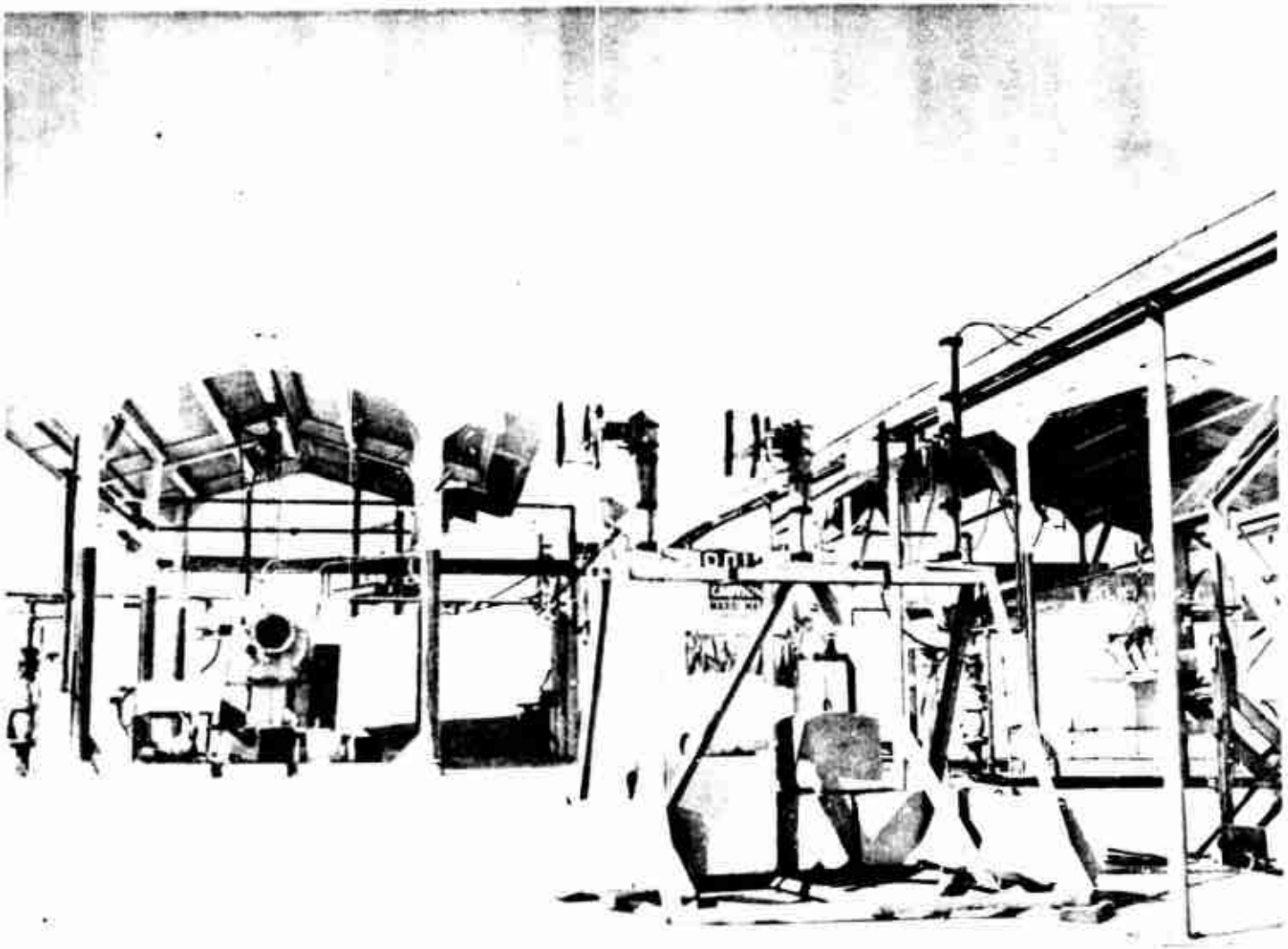

Figure 10. Diagonal Radar System

TABLE V. DIAGONAL ATTENUATION DATA

Propellant	Test	P (psi)	F (lbs)	Fuel Index	T_e (^oK)	D_t (in.)	r_j (in.)	ϵ	Attenuation (db) A	B	C
RHP-112	1*	1039	2019	0.63	1978	1.274	1.903	8.94	11.6	---	10.5
UTP-11475	2*	223	504	0.34	2908	1.488	1.345	3.19	2.5	3.4	3.8
UTP-11475	3*	225	519	0.34	2907	1.485	1.345	3.28	2.5	3.4	4.0
UTP-11475	4*	225	507	0.34	2907	1.484	1.340	3.20	2.2	4.0	4.1
AAP-3318	5**	586	2750	0.65	2311	2.014	2.321	5.310	16.5	15.7	14.0
AAP-3318	6**	575	2733	0.65	2311	2.013	2.318	5.319	14.9	13.5	12.5
AAP-3318	7**	599	2807	0.65	2311	2.013	2.311	5.307	15.7	14.8	13.3
AAP-3318	8**	609	2855	0.65	2311	2.012	2.316	5.306	15.8	14.3	12.8
AAB-3220	9**	325	2250	0.61	2372	2.526	2.440	3.741	16.7	15.9	15.0
AAB-3220	10**	602	3186	0.61	2311	2.122	2.392	5.124	16.8	16.1	15.2
AAB-3220	11**	962	4194	0.61	2202	1.870	2.737	8.57	16.8	16.0	15.5

* 15 lb test motor.

** 70 lb test motor.

SECTION IV

RADAR ADDITIVE TEST STUDY

Apparatus

The radar additive test study (RATS) was a low cost method of screening potential radar attenuation suppressants in a reasonably sized test motor. A diagram of the motor is given in Figure 11, a typical test firing is shown in Figure 12. One to three 30 lb layers of uncured propellant, each containing a different additive, were vacuum cast into the motor. A sharp interface between layers was obtained by freezing the surface of each layer before casting the next. Thus, a number of additives could be evaluated in each firing.

The K-band radar system was used to determine transverse attenuation at the exit plane of the motor. This measurement gives some indication of plume electron density before the afterburning of combustible gaseous exhaust species and alkali metal ionization. The X-band system was used to determine attenuation of a signal transmitted diagonally through the afterburning region of the plume. The evaluation of an additive is based on its suppression of attenuation in this region of greatest electron density. Further information concerning the RATS system may be found in AFRPL-TR-68-219.

Results

Partial results of the first additive study were presented in AFRPL-TR-68-219. That study was completed and all test data are presented in Appendix A.

Test data from the most recent additive study are presented in Tables VI and VII. The two baseline RATS formulations (no additives) are identical in propellant ingredients and solids loading. However, the

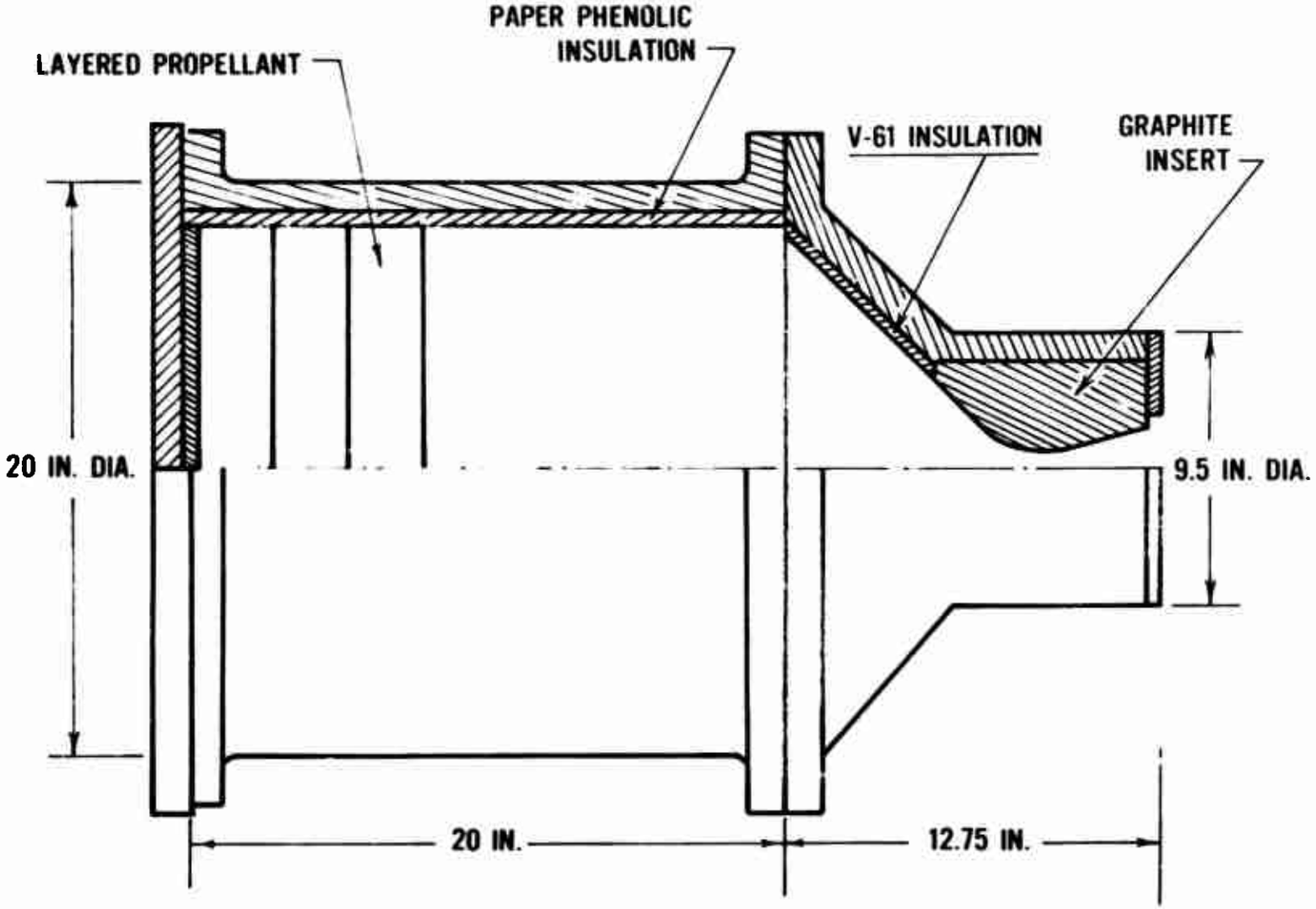

Figure 11. RATS Motor

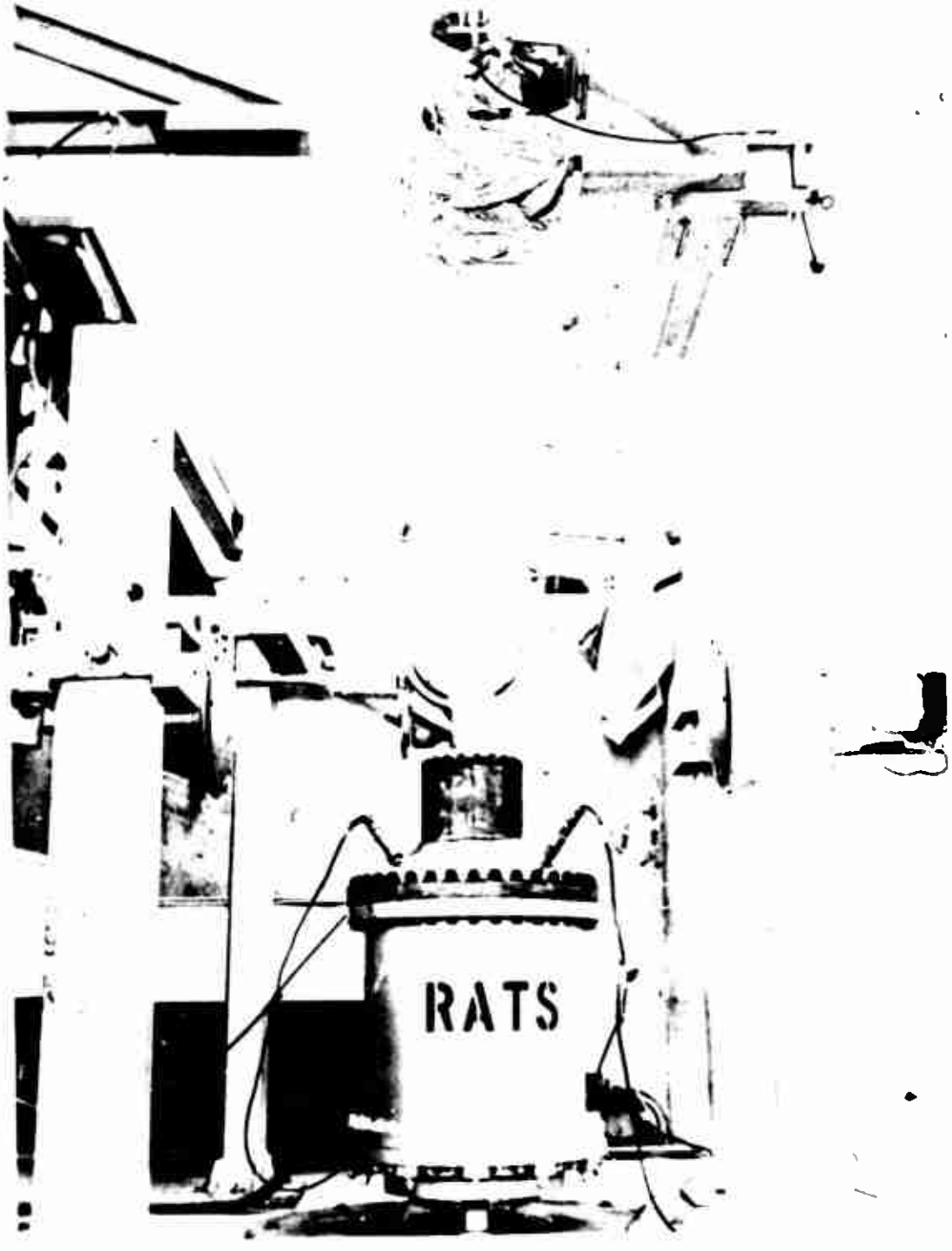

Figure 12. RATS Motor Firing.

level of Al and AP varies in these formulations as shown in Table III. The level of impurities present in both propellants for each of the additives is shown in Table VIII.

X-band attenuation with the 7-percent Al baseline formulation (no additive) was 1.1 db. An 82-percent reduction in attenuation (a reduction of 0.9 db) was achieved with 3-percent Mo and with 3-percent $VOSO_4$. Potassium sulfate, evaluated as a potential afterburning quencher, enhanced the attenuation to approximately 7 db (approximately a 540 percent increase) at the 3-percent additive level.

X-band attenuation with the 16-percent Al baseline formulation was 2.5 db. Attenuation was reduced 36 percent with the 3-percent $CoSnO_3$ formulation. A 40-percent reduction in attenuation was attained with 3 percent Cr_2O_3 and $VOSO_4$. Boron carbide effected the greatest reduction (56 percent) in attenuation with the 16-percent Al formulation. No data were obtained for the 3-percent Mo formulation; however, the 1-percent Mo formulation suppressed attenuation by 40 percent.

The additives are presented in order of decreasing effectiveness in Tables VI and VII. The theoretical loss in specific impulse caused by the additives indicates that a tradeoff between propellant performance and attenuation suppression is necessary. However, it should be noted that the use of the most efficient additive does not result in the greatest loss in specific impulse.

TABLE VI. ADDITIVE STUDY RESULTS
RATS 7% Al PROPELLANT

Additive	X-Atten (db)	P_c (psi)	ISP Loss (sec)*
None	1.1	662	0
1% Mo	0.3	730	1.3
1% $VOSO_4$	0.4	671	--
1% $CoSnO_3$	0.4	738	--
1% Cr_2O_3	0.4	560	1.6
1% $PbCrO_4$	0.5	659	1.2
1% B_4C	0.7	677	0.5
1% CuO	0.9	695	1.4
1% Pb	0.9	670	1.3
1% K_2SO_4	5.1	614	1.5
3% Mo	0.2	690	4.0
3% $VOSO_4$	0.2	707	--
3% $CoSnO_3$	0.3	681	--
3% Cr_2O_3	0.3	647	4.9
3% $PbCrO_4$	0.4	733	3.7
3% B_4C	0.5	624	0.8
3% CuO	1.2	742	4.2
3% Pb	1.3	665	3.9
3% K_2SO_4	6.9	683	4.6

* From Lockheed Theoretical Isp Program. Isp of RATS 7% Al baseline formulation = 249.7 sec.

TABLE VII. ADDITIVE STUDY RESULTS
RATS 16% Al PROPELLANT

Additive	X-Atten (db)	K-Atten (db)	P_c (psi)	Isp Loss (sec)*
None	2.5	0.4	548	0
1% Mo	1.6	1.0	552	1.5
1% B_4C	1.7	1.1	475	0.7
1% Cr_2O_3	1.8	0.6	477	2.0
1% $VOSO_4$	2.0	0.2	675	--
1% $CoSnO_3$	2.2	0.2	597	--
1% $PbCrO_4$	2.1	0.5	547	1.4
1% Pb	2.5	0.5	526	1.4
1% CuO	2.6	0.4	666	1.6
1% K_2SO_4	13.	3.2	549	1.6
3% Mo	--	--	--	4.4
3% B_4C	1.1	0.3	692	4.5
3% Cr_2O_3	1.5	0.5	493	5.6
3% $VOSO_4$	1.5	0.5	658	--
3% $CoSnO_3$	1.6	0.1	--	--
3% $PbCrO_4$	1.7	0.4	564	4.2
3% Pb	1.7	0.2	570	4.1
3% CuO	2.1	0.4	650	4.5
3% K_2SO_4	15.0	9.9	789	4.6

* From Lockheed Theoretical Isp Program. Isp of RATS 16% Al baseline formulation 260.1 sec.

TABLE VIII. RATS PROPELLANT IMPURITIES

Propellant	Additive	Na (PPM)	K (PPM)
7% Al	None	76	58
	1% Pb	76	56
	3% Pb	78	57
	1% Cr_2O_3	71	54
	3% Cr_2O_3	70	58
	1% CuO	75	55
	3% CuO	74	60
	1% K_2SO_4	88	1270
	3% K_2SO_4	118	3653
	1% $PbCrO_4$	71	54
	3% $PbCrO_4$	70	49
	1% $CoSnO_3$	77	57
	3% $CoSnO_3$	76	54
	1% B_4C	70	52
	3% B_4C	72	51
	1% $VOSO_4$	74	51
	3% $VOSO_4$	77	56
	1% Mo	76	54
	3% Mo	73	55

TABLE VIII. RATS PROPELLANT IMPURITIES (Cont'd)

Propellant	Additive	Na (PPM)	K (PPM)
16% Al	None	63	55
	1% Pb	56	56
	3% Pb	62	56
	1% Cr_2O_3	60	55
	3% Cr_2O_3	61	58
	1% CuO	62	61
	3% CuO	58	57
	1% K_2SO_4	72	1516
	3% K_2SO_4	--	--
	1% $PbCrO_4$	58	60
	3% $PbCrO_4$	58	60
	1% $CoSnO_3$	72	54
	3% $CoSnO_3$	77	57
	1% B_4C	67	62
	3% B_4C	55	54
	1% $VOSO_4$	64	59
	3% $VOSO_4$	65	58
	1% Mo	62	57
	3% Mo	60	52

SECTION V

SUMMARY OF RESULTS

1. Insufficient data were taken to allow definite conclusions to be drawn concerning the variation of peak transverse X- and K- band attenuation with chamber pressure, nozzle convergence angles and nozzle submergence. The data appear to indicate these variables have little effect on attenuation.

2. The attenuation caused by propellant UTP-11475 was significantly lower than any other propellant. This was due to a low fuel index and, hence, little afterburning.

3. The transverse attenuation by propellant AAB-3220 exceeded the limits of the system (20 to 25 db).

4. Diagonal X-band attenuation decreased approximately 2 db as the aspect angle increased from 14 degrees to 20 degrees. An exception to this was the UTP-11475 series, which was conducted at significantly lower chamber pressures.

5. X-band radar attenuation was significantly reduced in the 7-percent and 16-percent Al RATS formulations through the use of selected propellant additives. This reduction was accompanied by a decrease in the predicted specific impulse.

APPENDIX A

ADDITIVE STUDY RESULTS

	Additive	X- Atten (db) Trial No 1	2	K- Atten (db) Trial No 1	2	Pc (psi) Trial No 1	2
RATS Propellant 7% Al	None	1.3	0.8	---	0	710	710
	None	0.9	0.8	0	0	620	680
	1% Mo	0.9	0.2	---	0	740	802
	3% Mo	0.1	0.2	0	0	670	650
	1% W	0.3	0.2	---	0	740	652
	3% W	0.3	0.2	0	0	625	686
	1% Fe	0.2	0.2	0	0	616	623
	3% Fe	---	0.2	---	0	---	725
	1% Ni	0.4	0.5	0	0	545	654
	3% Ni	0	0	0	---	612	675
	1% B	0.6	0.5	---	0	920	675
	3% B	0.5	0.4	0	0	671	687
	1% S	0.2	1.0	---	0	815	675
	3% S	0.6	0.9	0	0	740	670
12% Al	None	1.9	1.7	0.4	---	800	670
	None	1.6	1.6	0	0	510	630
	1% Mo	0.7	0.6	0	---	612	666
	3% Mo	0.5	0.6	0	0	750	650
	1% W	0.8	0.5	0	0	564	562
	3 W	0.4	0.4	0	0	593	581
	1 Fe	0.6	0.6	0	0	556	565
	3 Fe	---	0.5	---	0	---	664

APPENDIX A

ADDITIVE STUDY RESULTS (Cont'd)

		Additive	X- Atten (db) Trial No 1	2	K-Atten (db) Trial No 1	2	Pc (psi) Trial No 1	2
RATS Propellant	12% Al	1% Ni	1.1	1.0	0.2	0.1	564	615
		3% Ni	0.8	0.7	0.1	0	607	632
		1% B	1.2	1.3	0.9	1.0	560	560
		3% B	1.0	0.9	0.8	0.9	760	635
		1% S	1.5	1.5	0	0	620	599
		3% S	1.5	1.3	0	0	626	603
	16% Al	None	1.9	3.2	0.7	1.5	700	715
		None	2.2	2.3	0.7	0.8	610	650
		1% Mo	1.5	1.4	0.4	0.5	695	684
		3% Mo	1.3	1.1	0.1	0.4	620	647
		1% W	1.3	1.5	---	0.8	700	815
		3% W	1.3	1.1	0.5	0.5	910	950
		1% Fe	1.8	2.1	0.5	0.7	698	730
		3% Fe	---	1.1	---	0.2	---	649
		1% Ni	1.7	1.4	0.2	0.2	581	620
		3% Ni	1.5	1.3	0	0	592	635
		1% B	1.7	1.8	0.7	---	645	640
		3% B	1.5	.5	0.5	0.6	720	791
		1% S	2.7	2.7	0.3	0.4	600	636
		3% S	2.0	2.3	0	0	630	674

APPENDIX A

ADDITIVE STUDY RESULTS (Cont'd)

		Additive	X- Atten (db) Trial No 1	X- Atten (db) Trial No 2	K- Atten (db) Trial No 1	K- Atten (db) Trial No 2	Pc (psi) Trial No 1	Pc (psi) Trial No 2
RATS Propellant	20% Al	None	2.7	2.8	0.6	0.6	580	575
		None	3.8	3.6	0.8	0.8	830	561
		1% Mo	3.5	3.5	0.7	0.6	736	786
		3% Mo	2.9	3.0	0.4	0.5	805	684
		1% W	3.4	3.5	0.6	0.6	830	790
		3% W	3.4	3.1	2.3	0.8	710	710
		1% Fe	2.9	3.1	0.3	0.4	759	766
		3% Fe	2.2	2.4	0.2	0.2	606	610
		1% Ni	2.8	3.2	1.2	1.0	560	670
		3% Ni	2.6	3.0	0.7	0.6	546	700
		1% B	2.2	2.3	---	0.5	580	620
		3% B	1.8	1.8	0.8	0.4	800	700
		1% S	3.8	2.4	0.7	0.4	800	650
		3% S	2.2	2.3	1.0	0.4	730	710

UNCLASSIFIED

Security Classification

DOCUMENT CONTROL DATA · R & D

(Security classification of title, body of abstract and indexing annotation must be entered when the overall report is classified)

1. ORIGINATING ACTIVITY (Corporate author) Air Force Rocket Propulsion Laboratory Edwards, CA 93523	2a. REPORT SECURITY CLASSIFICATION UNCLASSIFIED 2b. GROUP

3. REPORT TITLE

Radar Attenuation Measurements of Selected Solid Propellants and the Effect of Additives

4. DESCRIPTIVE NOTES (Type of report and inclusive dates)

Final Report

5. AUTHOR(S) (First name, middle initial, last name)

Laurice G. Altman
Samuel B. Thompson
Peter C. Sukanek

6. REPORT DATE	7a. TOTAL NO. OF PAGES	7b. NO. OF REFS
May 1973	36	0

8a. CONTRACT OR GRANT NO.	9a. ORIGINATOR'S REPORT NUMBER(S)
b. PROJECT NO. 305901 AMB	AFRPL-TR-73-29
c.	9b. OTHER REPORT NO(S) (Any other numbers that may be assigned this report)
d.	

10. DISTRIBUTION STATEMENT

Distribution limited to U.S. Gov't agencies only; test and evaluation; 15 Jan 73. Other requests for this document must be referred to AFRPL Office of Technical Information (DOZ), Edwards, California 93523.

11. SUPPLEMENTARY NOTES	12. SPONSORING MILITARY ACTIVITY
	USAF Rocket Propulsion Laboratory Edwards, CA 93523

13. ABSTRACT

The primary objective of Project EPIC was to characterize solid propellants with respect to radar attenuation by their plumes. This report presents transverse and diagonal radar attenuation data on four different solid rocket propellants: RHP-112, AAP-3318, UTP-11475 and AAB-3229. Transverse attenuation data for propellants containing each of nine different radar attenuation suppressants (Mo, B_4C, Cr_2O_3, $VOSO_4$, $CoSnO_3$, $PbCrO_3$, Pb, CuO, K_2SO_4) are also given.

DD FORM 1 NOV 65 1473

UNCLASSIFIED

Security Classification

14. KEY WORDS	LINK A		LINK B		LINK C	
	ROLE	WT	ROLE	WT	ROLE	WT
radar attenuation						
attenuation suppressants						
rocket exhaust plumes						

PROJECT SQUID

TECHNICAL REPORT ARC-8-P

TECHNIQUES FOR THE STUDY OF COMBUSTION OF BERYLLIUM AND ALUMINUM PARTICLES

By

A. Maček, R. Friedman, and J. M. Semple
Kinetics and Combustion Division
Atlantic Research Corporation
Alexandria, Virginia

DEPARTMENT OF AEROSPACE ENGINEERING
SCHOOL OF ENGINEERING AND APPLIED SCIENCE
UNIVERSITY OF VIRGINIA
CHARLOTTESVILLE, VIRGINIA

Project SQUID is a cooperative program of basic research relating to Jet Propulsion. It is sponsored by the Office of Naval Research and is administered by the University of Virginia through Contract Nonr 3623(00), NR-098-038.

February 1964

focal plane at a shallow angle. This system gives a magnification of film of 8 X. Satisfactory prints have been obtained with magnification factors up to 50. Positioning of the lens at various heights above the burner plate thus allows observation of the entire history of the particle from ignition to burnout.

b. Results

The photographic technique has been applied to combustion of spherical aluminum particles, size range of 30-35μ, and has revealed many complex features of the process. It had been found previously[2] that there are distinct effects on combustion of aluminum particles of both oxygen and water vapor in the hot ambient gases. Oxygen promotes vigorous combustion, and if its concentration is sufficiently high, there is fragmentation of burning particles. It had also been found that in virtual absence of water vapor there was much diffuse luminosity surrounding the burning particle, suggesting extensive vapor phase reaction, while in the presence of water in amounts larger than about 0.1 atm the luminous reaction is confined to a region closely adjacent to the particle. These effects have now been observed in close detail, as illustrated by Figures 5, 6, 7, 8, and 9.

Figures 5 and 6 show successive stsges of particle combustion in low-moisture and high-moisture gases respectively. The oxygen content in both cases is relatively low so that burning is smooth (no fragmentation). It can be seen that the stages in the two figures sre qualitatively similar. In the early stages following ignition, frames a and b in both figures, the burning appears even. The central intensely luminous core -- 30-50μ wide, corresponding approximately to the particle diameter -- is surrounded by a less luminous

TABLE OF CONTENTS

LIST OF ILLUSTRATIONS

LIST OF TABLES

Project SQUID Technical Report No. ARC-8-P

TECHNIQUES FOR THE STUDY OF COMBUSTION OF BERYLLIUM AND ALUMINUM PARTICLES*

A. Maček, R. Friedman, and J. M. Semple
Kinetics and Combustion Division
Atlantic Research Corporation, Alexandria, Virginia

ABSTRACT

Minimum ignition temperatures for single beryllium particles, under total pressures of up to 50 atmospheres, range from 2380° to 2650°K depending on the partial pressure of oxygen in the ambient gas. Atmospheric pressure photographic studies of fine details of aluminum combustion have also been made and are discussed qualitatively.

The work described herein deals with a fundamental investigation of ignition and combustion of single metal particles of diameters ranging from 30 to 45 microns. Although different experimental procedures have been used, the essence of this study has always been the same, and it is quite simple. Metal particles of known sizes and shapes are suddenly plunged into hot gases of known physical and chemical characteristics, and their behavior is observed.

Techniques needed for this work were to a large extent developed and used previously in a study of combustion of aluminum particles, and much of this development and application has been described in earlier publications.[1,2]

---

* This work was sponsored by Project SQUID which is supported by the Office of Naval Research, Department of the Navy, under contract Nonr 1858(25) NR-098-038. Reproduction in full or in part is permitted for any use of the United States Government.

The purpose of this paper is (1) to present the application of a previously developed technique to the study of beryllium particle ignition, and (2) to describe a recently developed technique for observation of fine details of metal particle burning which has so far been applied to aluminum only. Efforts are now being made to extend this technique to combustion of beryllium.

1. Ignition of Beryllium

a. Background

The main experimental problems in the study of beryllium ignition and combustion are the high ignition temperature of the metal and the high toxicity of both the metal and its combustion products. The combustion characteristics of the metal are largely determined by the thermodynamic properties of the metal and its oxide (BeO), listed in Table I. Since BeO forms a protective layer, one might expect, in analogy to the results previously obtained with aluminum,[1] that the ignition process will be influenced by the melting of beryllia. It is interesting to note that the normal boiling point of the metal is quite near the melting point of the oxide, and this may also be a determining factor in ignition. Indeed, as will be seen below, techniques necessary for a quantitative study of beryllium combustion must allow generation of controllable ambient temperatures approaching these high values. The boiling point of beryllia, about 4100°K, presumably determines the metal flame temperature.

b. Experimental Procedure

The procedure was to admix small amounts of the metal powder to a combustible mixture consisting of a fuel and an oxidizer, which was then burned

in loosely tamped powder form (about 1 gm/cc) in a pressurized bomb. The oxidizer was ammonium perchlorate. The fuel was trioxymethylene, a volstile compound, which makes even quite fuel-lean, relatively cool, mixtures flammable at atmospheric pressure. The smount of beryllium added, 0.05 per cent by weight, was so small that it did not perturb the thermodynsmic properties of the oxidizer-fuel mixture to any appreciable extent. A dilute stream of metal particles thus ignited and burned in the combustion product gases conaiating of known proportions of H_2O, CO_2, N_2, HCl, O_2, and free atoms and radicals. Temperature of the gases for several constant pressures wss computed by an IBM-7090 program with the usual assumption of equilibrium adiabatic conditions, and it was also measured, at atmospheric preasure, by the spectral line reversal method. The measured temperatures were 60 to 70°K below the computed ones.

Safe handling of beryllium and its combuation products presents a major problem. An appsratus conforming to stringent industrial hygiene requirements, shown in Fig. 1, has therefore been constructed which allows the beryllium-containing powder to be ignited in sealed capsules. Dilution required for diaposal of combustion producta ia 1 part of beryllium in s million parts of water or 25 micrograms of beryllium in one cubic meter of air. The combuation products contained in the sir-tight burner are therefore flushed first with a stream of nitrogen through dry filter, and then with generous amounts of water, all without opening the burner. Frequent analytical safety checks are necessary.

The procedure of determining the ignition limit aa a function of ambient gas temperature and oxygen content can be illustrated by reference to Fig. 2

which describes these ambien conditions corresponding to mixtures of ammonium perchlorate and trioxymethylene at three pressures; the percentage of free oxygen in the ambient gas is virtually independent of the total pressure so that a single oxygen-content curve suffices for all pressures. As long as the mixture is fuel-lean, progressive addition of fuel to oxidizer increases the temperature and decreases the oxygen content of the product gas. The procedure is continued up to the temperature at which a significant fraction of the metal particles ignite. This temperature and the corresponding partial pressure of oxygen are the ambient conditions which define the ignition limit of the metal.

c. Results

The results of ignition of beryllium particles, size range 30-45μ, are shown in Fig. 3. The total pressure in the above described experimental procedure is not an independently variable parameter, and it varies from point to point in the figure from 2.4 to 50 atmospheres. It can be seer that the metal ignites at temperatures as low as 2380°K when the partial pressure of oxygen is several atmospheres, and only above 2650°K when it is down to about 0.1 atm; this means that in fuel-rich mixtures the temperature limit for ignition of beryllium approaches the melting point of BeO (2820°K). Thus it appears possible that, in a close analogy to the case of aluminum, the temperature of the beryllium particle rises by self-heating above the ambient temperature to the melting point of the oxide, at which point ignition occurs. Since the normal boiling point of beryllium is slightly below the melting point of the oxide, boiling of the metal introduces an additional process to reckon at low pressures. Further work, which is in progress now, may give

basis for firmer judgment.

The mode of combustion of beryllium particles was also found to be affected by the ambient conditions. Large excess of oxygen appears to accelerate the burning. At low oxygen content, low pressures, and high temperatures, metal particle tracks are sharp and straight on photographic exposures, a characteristic of surface combustion of metals. At high oxygen content, high pressures, and low temperatures, the light from the burning particle is often intermittent and fairly diffuse, characteristic of gaseous combustion. These trends are illustrated by photographs taken through the window of the closed bomb (Fig. 4).

2. Photographic Study of Particle Combustion

a. Experimental Technique

In this technique metal particles are injected into laminarly flowing hot gases, generated by a flat-flame burner. The burner and the properties of the gases it generates were described in detail before.[1,2] Briefly, the hot gases consist of known proportions of H_2O, CO_2, N_2, and O_2, which are independently variable to a significant extent; the temperature can be varied from 1900 to 2800°K; the total pressure is restricted to 1 atmosphere.

The diagnostic technique for studying fine details of particle combustion consists of still photography through a magnifying lens system. The optical system has a standard 48 mm focal-length objective lens and a 10X magnifying eyepiece. Photographs are taken by a Reflex Leitz Microscope camera using 35 mm TRI X film. The depth of focus is 0.5 mm and the field of view 4.5 mm. The optical system is mounted on a cathetometer at a slight angle off the horizontal so that the vertically rising particles cross the

focal plane at a shallow angle. This system gives a magnification of film of 8 X. Satisfactory prints have been obtained with magnification factors up to 50. Positioning of the lens at various heights above the burner plate thus allows observation of the entire history of the particle from ignition to burnout.

b. Results

The photographic technique has been applied to combustion of spherical aluminum particles, size range of 30-3μ, and has revealed many complex features of the process. It had been found previously[2] that there are distinct effects on combustion of aluminum particles of both oxygen and water vapor in the hot ambient gases. Oxygen promotes vigorous combustion, and if its concentration is sufficiently high, there is fragmentation of burning particles. It had also been found that in virtual absence of water vapor there was much diffuse luminosity surrounding the burning particle, suggesting extensive vapor phase reaction, while in the presence of water in amounts larger than about 0.1 atm the luminous reaction is confined to a region closely adjacent to the particle. These effects have now been observed in close detail, as illustrated by Figures 5, 6, 7, 8, and 9.

Figures 5 and 6 show successive stages of particle combustion in low-moisture and high-moisture gases respectively. The oxygen content in both cases is relatively low so that burning is smooth (no fragmentation). It can be seen that the stages in the two figures are qualitatively similar. In the early stages following ignition, frames a and b in both figures, the burning appears even. The central intensely luminous core -- 30-50μ wide, corresponding approximately to the particle diameter -- is surrounded by a less luminous

region. The striking difference between Figures 5 and 6 is the appearance of the outer region, which is much wider and more diffuse in the absence of water. This difference in appearance persists into the later stages (Fig. 5c and 6c) in which the particles rotate. Fig. 6d records a particle at or near burnout; rotation has ceased, there is no outer region, and luminosity of the central core is dwindling. These progressive stages are typical of burning aluminum particles in hot gases whose oxygen content is too low to cause fragmentation.

Figures 7, 8 and 9 show comparable phenomena in high-moisture and low-moisture gases, side by side. The temperature in these figures is about 2400°K, and there is sufficient oxygen to cause some particles to undergo fragmentation (Fig. 9). The difference in the amount of diffuse luminosity between the adjacent photographs differing in amounts of water vapor is quite pronounced in all three figures.

There does not seem to be a ready explanation for these complex processes. However, we found in our earlier work[2] that, while in the presence of appreciable amounts of water vapor combustion of aluminum particles is accompanied by formation of hollow bubbles (reported earlier by Fassell et al[3]), there is no evidence of such a process in low-moisture gases. This fact and the fact that in the presence of water vapor the outer, less luminous, region is sharply delineated on the outside (e.g. Figures 6b and 7b), suggest that the outer layer luminosity may represent different things. In the presence of water, where combustion is confined to a region close to the surface and takes place asymmetrically with formation of bubbles, the dim outer layer is perhaps a relatively cool condensed phase portion of the burning system. In

the absence of water the burning is probably true vapor phase reaction, which indeed one should expect for aluminum on the basis of the relative volatilities of the metal and the oxide.[4]

Work is now in progress to apply the gas-burner photographic techniques to combustion of beryllium particles.

References

1. R. Friedman and A. Maček, Combustion and Flame, 6, 9 (1962).

2. R. Friedman and A. Maček, Ninth Symposium (International) on Combustion, pp 703-712. Academic Press, 1963.

3. W. M. Fassell, C. A. Papp, D. A. Hildenbrand, and R. P. Sernka, Solid Propellant Rocket Research, pp 271-278. Academic Press, 1960.

4. I. Glassman, 14th Annual Meeting of American Rocket Society, Washington, D. C., November 16-20, 1959.

TABLE I

Thermodynamic Properties of Be and BeO

(JANAF Thermochemical Data)

	Be	BeO
Melting point (^{o}K)	1556	2823
Boiling point (^{o}K)	2757	(4123)
Heat of fusion (kcal/mole)	2.8	(14)
Heat of Vaporization (kcal/mole)	71.1	(143.5)
Density (gm/cc)	1.82	3.02

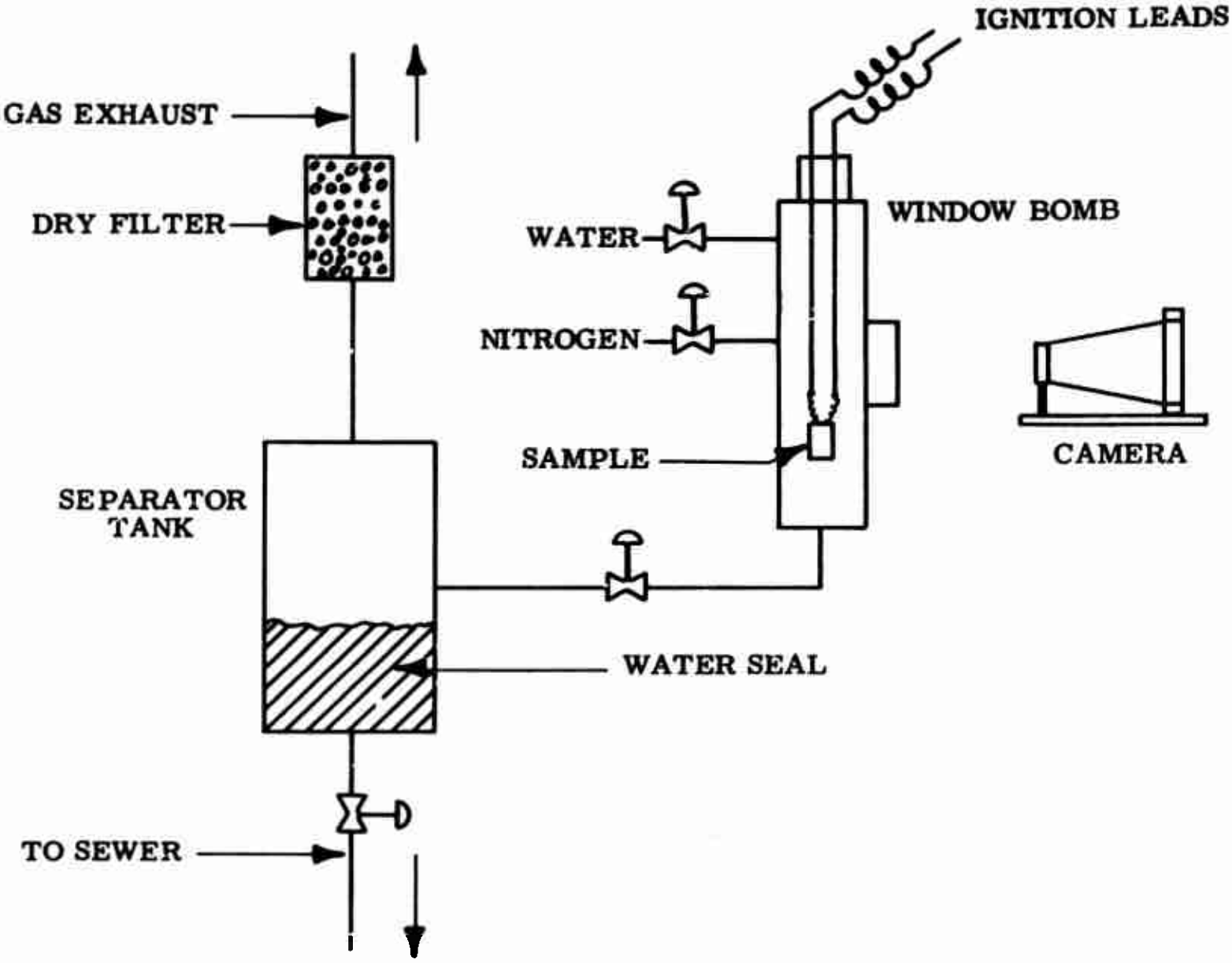

Fig. 1 APPARATUS FOR COMBUSTION OF BERYLLIUM UNDER PRESSURE

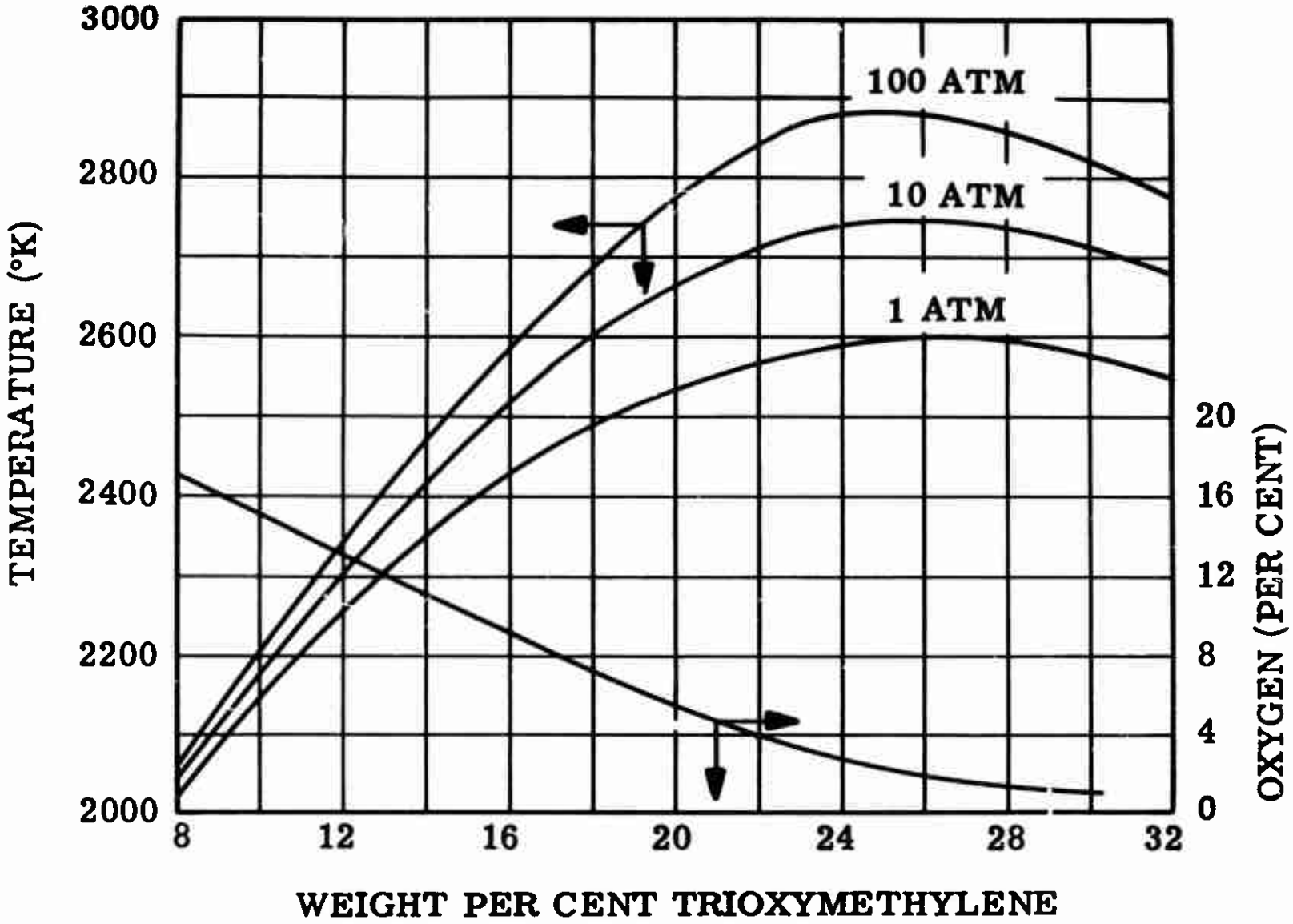

Fig. 2 CALCULATED ADIABATIC FLAME TEMPERATURE OF AMMONIUM PERCHLORATE-TRIOXYMETHYLENE MIXTURES AT SEVERAL PRESSURES

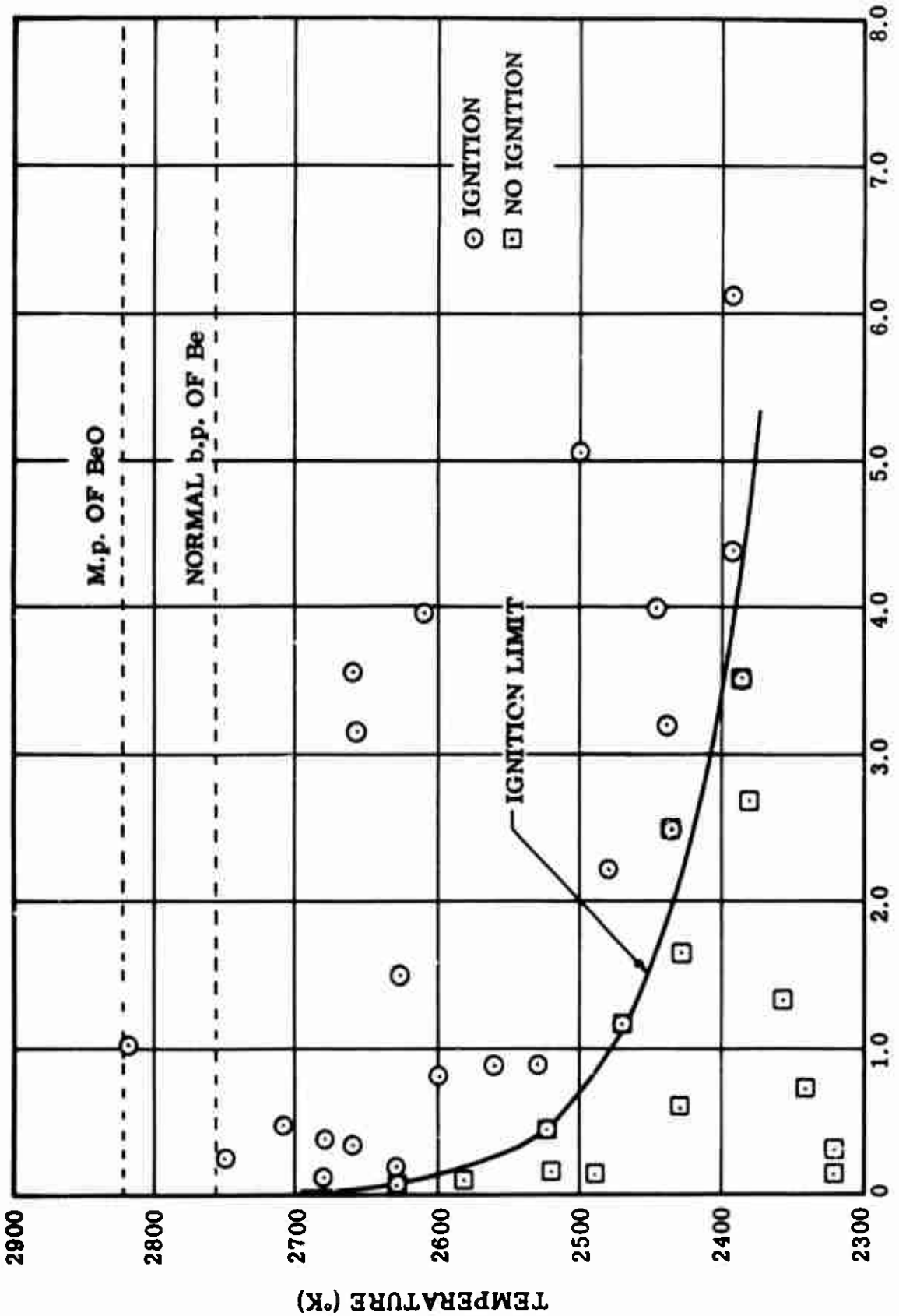

IGN'TION OF BERYLLIUM PARTICLES (DIAMETER RANGE 30-45 MICRONS)

Fig. 3.

13% $C_3H_6O_3$

87% NH_4ClO_4

T = 2380°K

O_2 Partial Pressure = 6.12 Atm.

700 # psig

21.5% $C_3H_6O_3$

78.5% NH_4ClO_4

T = 2660°K

O_2 Partial Pressure = 0.335 Atm.

100 # psig

Fig. 4. COMBUSTION OF BERYLLIUM PARTICLES IN A CLOSED BOMB

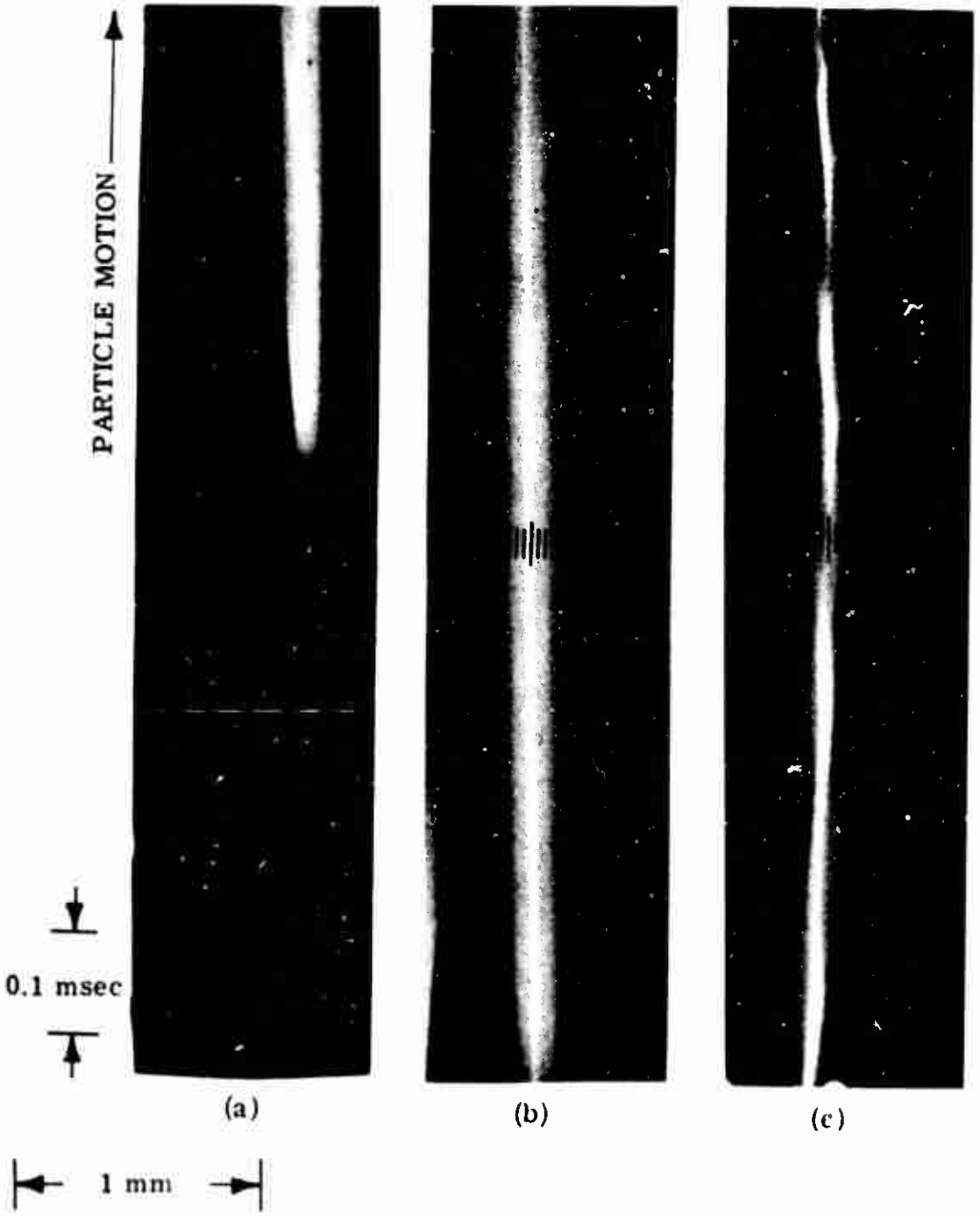

Figure 5. Time exposure of vertically moving, burning single Al particles, diameter range 30-35μ. Ambient gas properties: T = 2530 K, O_2 = 7.9%, H_2O = 0.5%. Residence time of particle in gas is:

(a) 10.4 msec to 11.4 msec (ignition at 11.0 msec)
(b) 11.8 msec to 12.8 msec
(c) 13.2 msec to 14.2 msec (near burnout)

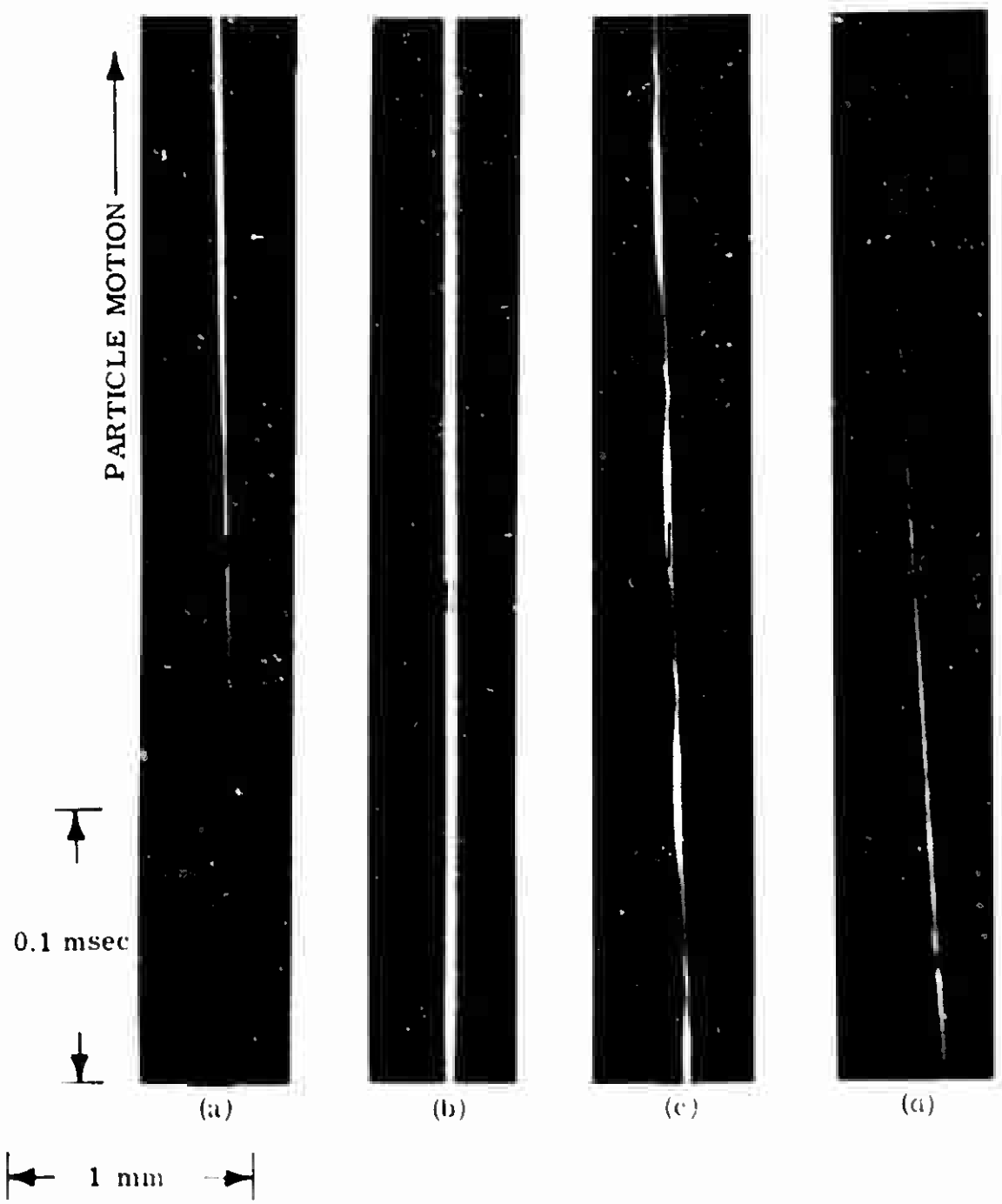

Figure 6. Time exposure of vertically moving, burning single Al particles, diameter range 30-35-. Ambient gas properties: T 2500 K, O_2 15.8%, H_2O = 17.4%. Residence time of particles in gas is:

(a) 7.5 msec to 7.9 msec (ignition at 7.6 msec)
(b) 8.6 msec to 9.0 msec
(c) 9.7 msec to 10.1 msec (rotation)
(d) 10.8 msec to 11.2 msec (near burnout)

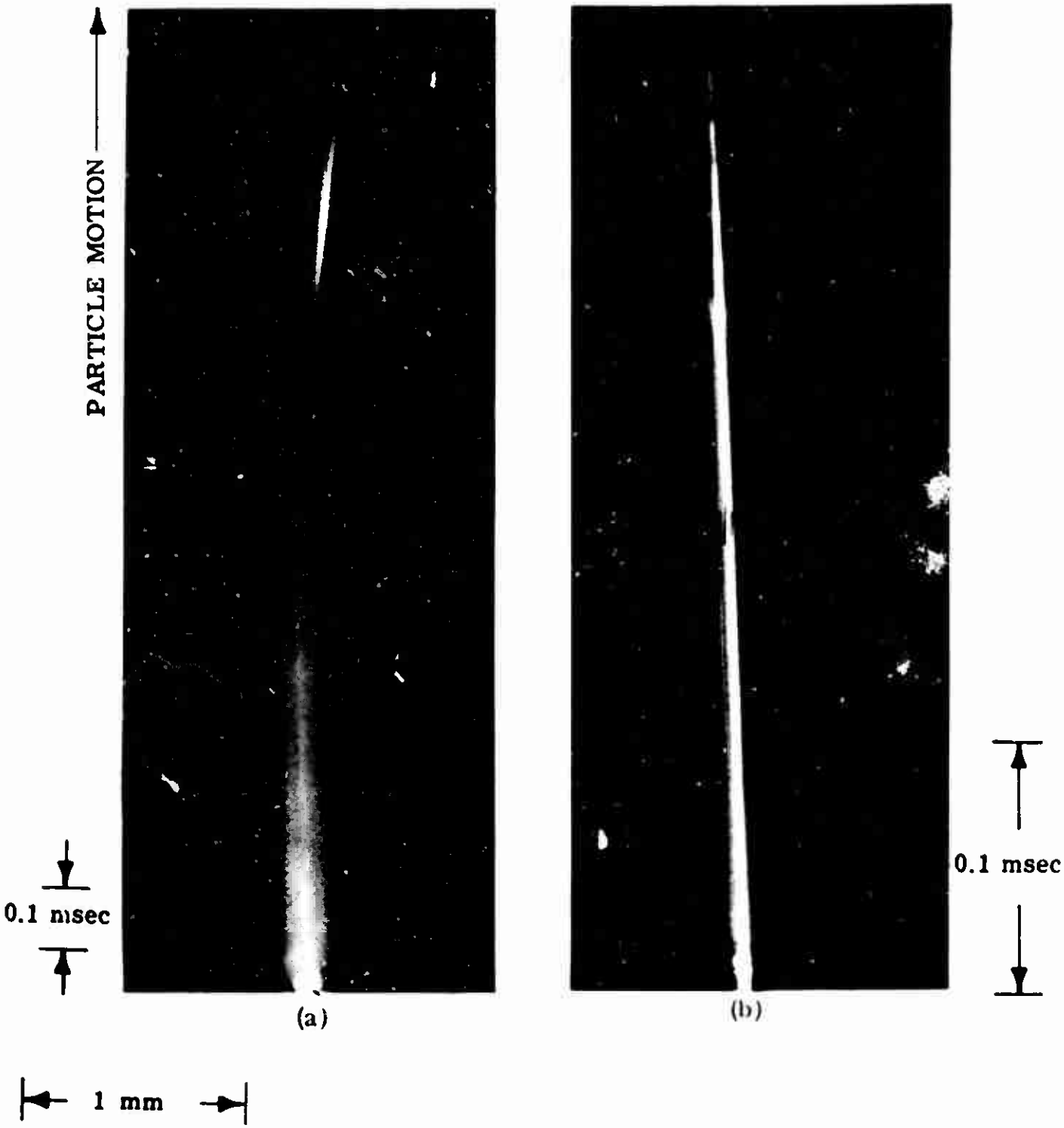

Figure 7. Time exposure near burnout of vertically moving, single Al particles, diameter range 30-35-, burning in gases with following properties:

(a) T = 2390 K, O_2 = 34%, H_2O = 0.6%
(b) T = 2410 K, O_2 = 32%, H_2O = 17%

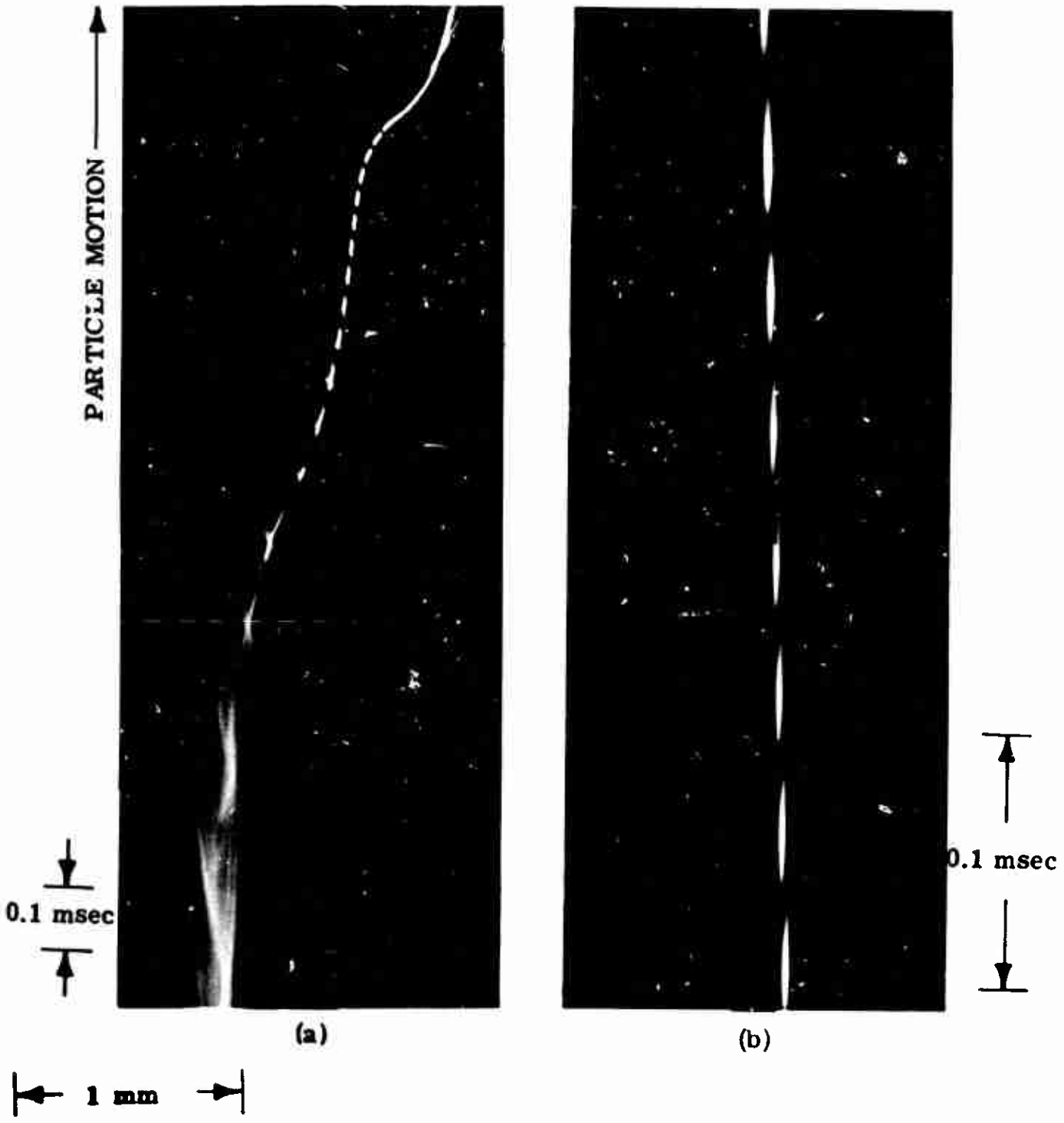

Figure 8. Time exposure of vertically moving, rotating, single Al particles, diameter range 30-35μ, burning in gases with following properties:

(a) T = 2390°K, O_2 = 34%, H_2O = 0.6%
(b) T = 2410°K, O_2 = 32%, H_2O = 17%

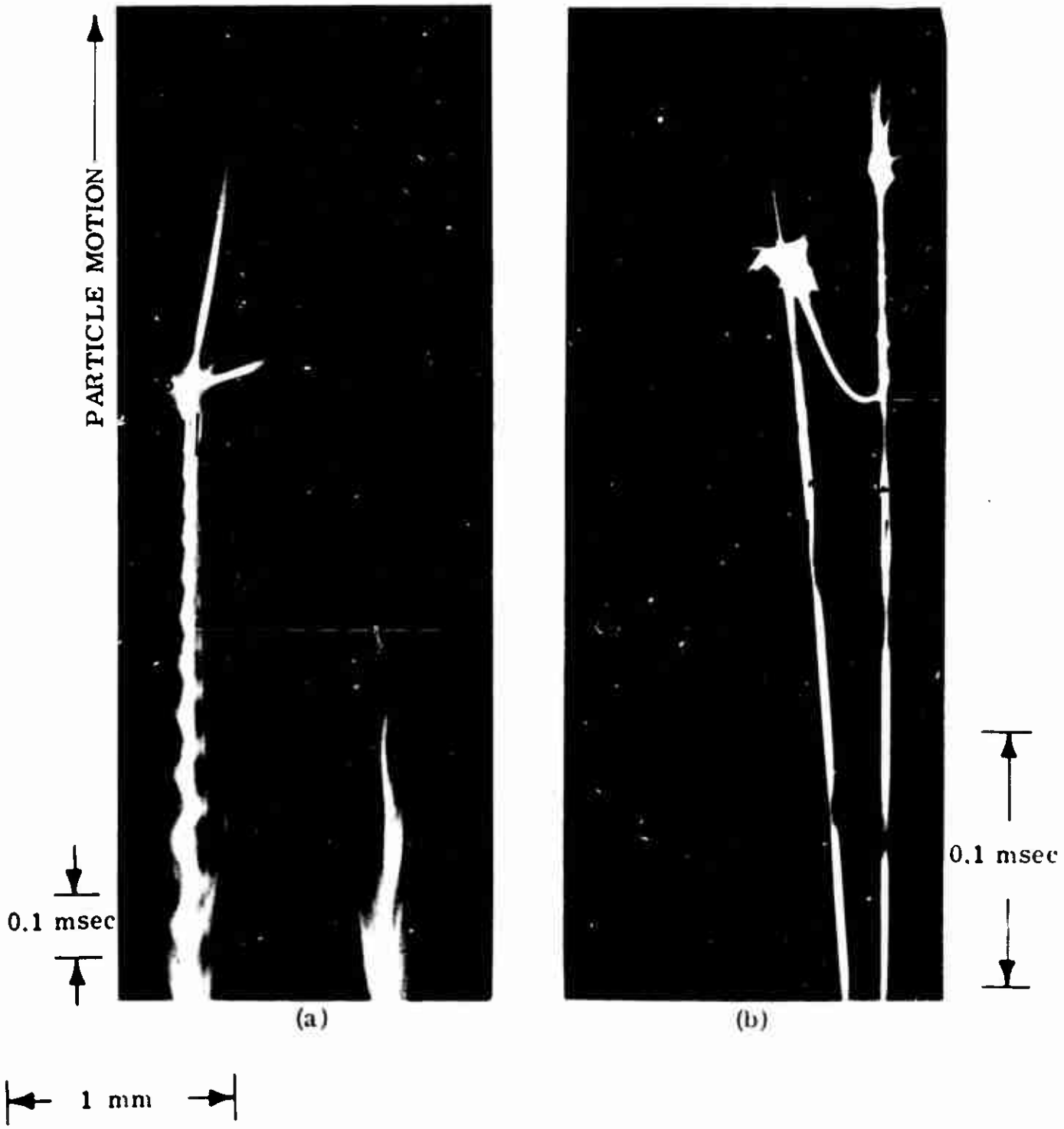

Figure 9. Time exposure at burnout (with fragmentation) of vertically moving single Al particles, diameter range 30-35-, burning in gases with following properties:

(a) T = 2390 K, O_2 = 34%, H_2O = 0.6%
(b) T = 2410 K, O_2 = 32%, H_2O = 17%

END

FILMED

11-83

DTIC